E-2040

TN-8, TN-8L AND TN-9

SAFETY ANALYSIS REPORT

Volume 2

Revision 12
December 27, 1990

Transnuclear, Inc.
Two Skyline Drive
Hawthorne, N.Y. 10532

9104090092 910325
PDR ADOCK 07109015
B PDR

TABLE OF CONTENTS

	Page
INTRODUCTION - General Information And Dry Shipment Considerations	1
CHAPTER I - Description And Charateristics Of The Irradiated Fuel Assemblies	7
1. Generalities	7
2. Main Characteristics Of The Fuel Assemblies	8
3. Characteristics Of Irradiation And Cooling	11
4. Residual Power Of The Fuel Assemblies	11
5. Activity Of The Fuel Assemblies	13
6. Fission Products	15
7. Risk Of Damage To The Irradiated Fuel Assemblies Under Normal And Accidental Conditions Of Transport	20
CHAP II - Description and Construction Characteristics Of TN8 and TN9 Packaging Designs	30
1. General Description	30
2. Detailed Description	32
Annex A To Chapter II - Characteristics Of Materials	42
1. Carbon Steel	42
2. Austentic Stainless Steel	42
3. Steels Used for Screws	42
4. Lead	43
5. Copper	44
6. Resin	44
7. Cement	45b
8. Balsa Wood	45c

9. Boron Carbide And Copper Sintered Plates 46
10. Gaskets 47
11. Polyamide Resin 47

Annex B to Chapter II - Applicable Fabrication Code And Special Fabrication And Inspection Procedures 48

1. Fabrication Code 48
2. Welds 48
3. Leaktightness Test Of Sealed Chambers 49
4. Control Of Boron Contents And Positioning Of B4C-CU Plates 52
5. Lead Shielding Casting And Inspection 52b
6. Neutron Shielding Inspection 52c

Annex C to Chapter II - 53

1. Packaging Component Listing 53
2. Packaging Gasket Listing 54
3. Packaging Orifice Listing 55

Annex D to Chapter II - (Deleted) 55a

CHAP III - Conformity To Packaging And Package Requirements 60

1. General Design Requirements 60

2. Additional Requirements For Type A Package 62

3. Basic Additional Requirements For Type B (U) Packages 68

Annex A To Chapter III - Shield Calculations 73

1. TN8 Packaging 73
2. TN-9 Packagings 95
3. Dose Rates At 1 Meter From The Packaging After The Regulatory Tests (C-2.3.1.b) 109
4. Shielding Calculation For P1 and B1 Fuel Assemblies 110
5. Shielding Evaluation in the TN-8/8L Configuration x 110a

Annex B To Chapter III - Structural Resistance 112

1. Trunnions And Attachments 112
2. Lifting Lugs 119
3. Resistance To Dynamic Load Of The Screws Fixing The Lid And Orifice Flanges 120

4. Resistance Of The Packaging Cavity To Design Pressure 121

5. Stresses Of The Fuel Compartment Walls For An External Pressure Of 1 BAR 126

6. Resistance To Bending Of The Packaging Body 128

Annex C To Chapter III - Analysis Of Conformity To Regulatory Leakage Testing Requirements 131a

1. Maximum Permissible Leakage Rates (L_A) and (L_N) 131b
2. Containment System Design Verification 131r
3. Containment System Fabrication Verification 131r
4. Containment System Assembly Verification 131r
5. Containment System Periodic Verification 131s
6. Backfill Pressure at Closure 131t

CHAP IV - Conformity Of The Requirements Concerning The Heat Generated by Fuel Assemblies 132

1. General Considerations 132

2. Temperature Of The Accessible Surfaces Of The Packages 133

3. Temperatures Reached In The Various Constituents Of The Packages 134

4. Analysis of Possible Damage To The Packagings 139

5. Temperature Reached In The Fuel Assemblies 141

6. Average Gas Temperature 152

7. TN-8L Heat Transfer 152

8. Thermal Evaluation of TN-8 and TN-8L with PP Fuel 152

Annex A to Chapter IV - Equilibrium Temperatures Of The Full Scale Model Representing A Cross-Section Of The TN9 Packaging

1. Introduction 153
2. Results Of TN9 Cross Section Test 153
3. Results Of The Thermal Tests Concerning Prototypes Of TN8 And TN9 Packagings 157

Annex B To Chapter IV - Temperatures Reached By The Pins In A Scale-Model Simulating A "P" Assembly And Placed In A TN8 Fuel Housing 161
1. Introduction 161
2. Description Of Apparatus 161
3. Results Of Measurement 163
4. Interpretation Of Experimental Results And Application To "P" Assemblies 164

Annex C To Chapter IV - Effective On Radiative Thermal Dissipation Caused By Substitution Of The Nickel-Chromium Coating For Paint On TheCooling Fins Of The TN8/TN9 Packagings 168a
1. Introduction 168a
2. Evaluation Of The Heat Dissipated By Radiation During The Thermal Tests Of TN8/TN9 Prototypes. 168a
3. Effect On Heat Dissipation By Radiation Caused By Changing The Emissivity Coefficient Of The Fins 168d

Annex D To Chapter IV - Temperature Of The Fuel Compartments 168k
1. Objective 168k
2. TN9 Packaging 168k
3. TN8 Packaging 168a

Annex E To Chapter IV - Thermal Stress Analysis 168u
1. Objective 168u
2. Thermal Stresses Related To The Radial Differential Expansion In A Packaging Cross Section 168u
3. Thermal Stresses In The Drain Lines 168w
4. Conclusion 168z8

CHAP V - Conformity Under Regulatory Test Conditions 169

1. Tests Common To Type A And B Packagings 169

2. Tests Specific To Type B Packaging 170

3. Fire Test 178

4. Conclusions 183

Annex A To Chapter V - Drop Tests Of TN9 Cask Quarter Scale Model 184
1. Introduction 184
2. Description Of The Package 184
3. Fuel Rod Characteristics 186
4. Test Facility 186
5. Drop Tests 186
6. Inspection Of Model After The Tests 187
7. Discussion 188

Annex B To Chapter V - Drop Tests For Half Scale Model 194a
1. Introduction 197
2. Description Of Model 198
3. Test Procedure 199
4. Test Results 201
5. Acknowledgements 207

Annex C To Chapter V - Fire Test For Half Scale Model 207a
1. Introduction 211
2. Description Of Model 212
3. Theory Of Scale Modeling 216
4. Computed Performance 219
5. Preparation For Fire Tests 230
6. Performance Of Test 232
7. Results Of Fire Test 235
8. Summary And Conclusions 239
9. Acknowledgements 241

Annex D To Chapter V - Fire Test Of TN9 Full Scale Slice 259

1. Introduction 259
2. Brief Description Of Facilities 259
3. Description Of Model 260
4. Test 261
5. Results 261
6. Conclusion 263

Annex E To Chapter V - Drop Test Evaluation 265a
1. Objective 265a
2. Horizontal Drop Of 9 Meters On The Trunnions 265a
3. One Meter Drop On A Punch 265n
4. Behavior Of The TN9 Fuel Compartments In The Conditions Of The 9 Meters Drop 265p
5. Behavior Of The TN8 Fuel Partitions In The Conditions Of The 9 Meters Drop 265u

6. TN-8L Structural Evaluation, Accident Conditions 265y

CHAP VI - Deleted

CHAP VII - Conformity to Requirements Specific to Fissile Class II Packages 269

1. Maintenance of the Essential Characteristics of the packages under the Conditions Specified in 709 to 714 - Section VII of 2 - 615 269
2. Individual Package Considered in Isolation 270a
3. Assemblies of Packages 271

Annex A to Chapter VII-Microscopic Cross Sections as a Function of Neutron Energy 276

Annex B to Chapter VII-Validity of the Apollo and Moret Calculation Methods 277

1. Lattice of UO2 Pins with Variable Square Pitch Submerged in Water 277
2. Parallel piped Core of UO2 Pins in Water (32) 277
3. Conclusion 277a

Annex C to Chapter VII - Data and Criticality Calculations Concerning the TN8 and TN8L Packaging 278

1. Data Concerning the Packaging and Contents 278
2. Safety of an Isolated Package 278
3. Normal and Accidental Transport Conditions 281a
4. Conclusions 282

Annex D to Chapter VII - Data and Criticality Calculations Concerning the TN9 Package 285b

1. Data Concerning the Package Contents 285b
2. Calculations of Keff of a Packaging in Water 286
3. Safety of an Isolated Packaging 289
4. Safety of the Packaging Under Normal Conditions and Transport Accidents 290
5. Conclusions 290

Annex E to Chapter VII - Criticality Evaluation for Stainless Steel Clad Fuel and Arrays of LWR Fuel Rods 290b

CHAP VIII - Packaging Acceptance, Operations and Maintenance Programs 290q

1. Acceptance Program 290q

2. Operations 293

3 Maintenance Program 196

Annex A To Chapter VIII - Handling Attachment Testing 299
1. Test Specifications 300
2. Acceptance Criteria 301
3. Corrective Action 302

Annex B To Chapter VIII - Hydraulic Test 303
1. Design Conditions And Minimum Test Pressure 303
2. Test Procedure 303
3. Acceptance Criteria 304
4. Corrective Action 304

Annex C To Chapter VIII - Leakage Test For Containment System Fabrication Verification 305

Annex D To Chapter VIII - Leakage Test For Lid Gasket Interspace 307

Annex E To Chapter VIII - Thermal Testing 308
1. Test Procedure 308
2. Test Duration 309
3. Measurement 309
4. Acceptance Criteria 310
5. Corrective Actions 310

Annex F To Chapter VIII - Draft Loading Instruction 311
1. Acceptance And Off-Loading Cask 311
2. Loading 313
3. Preparation For Cask Release 314
4. Preparation For Cask Shipment 316

Annex G To Chapter VIII - Draft Unloading Procedure 319
1. Acceptance And Off-Loading Cask 319a
2. Unloading 322
3. Preparation For Cask Release 322
4. Preparation For Cask Shipment 323

Annex H to Chapter VIII - Operating Instructions Referenced Figures 327

Annex I To Chapter VIII - Procedure For Drying The Package Cavity 339
1. Reasons for Drying the Cask Cavity of A Loaded Package 339
2. Basic Principles of Drying Procedure 340
3. Drying Procedure 340

Annex J To Chapter VIII - Leakage Test for Containment Assembly Verification 342
1. Procedure for Testing Package Cavity Leaktightness 342
2. Acceptance Criteria and Test Sensitivity 342
3. Corrective Actions 342
4. Procedure for Testing Lid Closure Tightness 343

Annex K to Chapter VIII - Keff Verification 344
1. Principle 344
2. Procedure 345
3. Acceptance Criteria 346
4. Corrective Action 346

Annex L to Chapter VIII - Heat Dissipation Capability Verification 347

Annex M to Chapter VIII - Shielding Efficiency Verification 348
1. Procedure 348
2. Acceptance Criteria 348
3. Corrective Action 348

Annex N to Chapter VIII - Packaging, Acceptance, Operations and Maintenance Programs - Configuration X Lid 349a

CHAP IX - Bibliography 350

Drawings

TN-8 Packaging (9317.01, Rev. J) 353

TN-9 Packaging (9317.03, Rev. J) 354

TN-8L Packaging (9317-138, Rev.A) 355

Configuration X Lid (9040-500-1, Rev. 1) 356

Configuration X Lid (9040-500-2, Rev. 1) 357

Configuration X Lid (9040-500-3, Rev. 0) 358

LIST OF FIGURES AND DRAWINGS

Figure or Drawing		Page
1-1	Cross-Section of a "P" Fuel Assembly	29
1-2	Cross-Section of a "B" Fuel Assembly	29
2-1	TN8 Packaging Over View	41
2-2	TN9 Packaging Over View	41a
2-3a	TN8 Packaging	41b
2-3b	TN9 Packaging	41c
2-5	TN8 Packaging 1/2 Cross-Section and Inner Shell Detail	41d
2-6	TN9 packaging 1/2 Cross-Section	41e
2-7	Lid Comparison	41f
3-A-1	Line Source	111
3-A-2	Reduction of Shielding	111
3-A-3	Extremity Shielding	111
3-A-4	Three "P" Assemblies Source	111
3-A-5	Evaluation of Gamma Source	111
3-A-6	Source and Shield Configuration for Dose Rate on Shock Absorbing Cover	111a
3-A-7	Source and Shield Configuration for Dose Point on Drum, Elevation	111b
3-A-8	Source and Shield Configuration for Dose Point on Drum, Plan View	111c
3-B-1 a-b-c	Vertical Handling	130
3-B-2 a-b-c-d	Stresses in the outer shell	130a
e-f-g	" " "	130b
3-B-3 a-b-c-d	Horizontal transport	130c
3-B-4 a-b-c-d-e	" "	130d
3-B-5,6,7,8	Lifting lugs and bending stresses in the outer shell and lead	130e
3-B-9,10,11,12 13,14,15	Stresses in lateral walls, bottom plate lid lodgement and lid bottom plate	131
4-1,4-2	TN8 and TN9 Temperature Profiles	152a
4-3	TN-8L Temperature Profile	152g
DWG 9085-69	TN9 Section for Thermal Test	158
4-A-1,2,3	Thermal Tests on Model	159
4-A-4	TN9 Thermal Model - External View Showing Lateral Insulation	160
4-A-5	TN9 Thermal Model Without Lateral Insulation	160
4-B-1	Temperature Distribution in "p" Assembly Model	167
4-B-2	Heating Array Temperature vs. Wall Temperature	167
4-B-3	Variation of Heating Array Temperature With Respect to Heat Flux Under Normal and Accidental Transport Conditions	167
4-B-4,5	Electrically Heated Bundle Simulating a Section of a PWR Fuel Assembly at scale 0.643	168

Figure or Drawing		Page
4-C1-C2-C3-C4	Thermal Emission and Reflexion in the Fins	168j
4-D1	TN9 Cavity	168s
4-D2	TN8 Cavity	168t
4-E1-4	Drain Line Configuration	168z10
4-E-5	Drain Line Connection Temperature Profile	168z11
5-1,2,3	Fire Condition Temperatures	183b
DWG 9085-44	Quarter-Scale Model	189
5-A-1	Quarter Scale Model Before Tests	190
5-A-2	Deformation After Second 9 Meter Drop	190
5-A-3	Deformation after 9 Meter Drop on Rear Cover	190
5-A-4	Condition After Ninth Drop (20 Meter Drop)	190
5-A-5	Condition of Lid and Housing After Ninth Drop	191
5-A-6	Section Through Model Bottom Showing Collapsed Trunnion	191
5-A-7	Longitudinal Section through Cask Body	191
5-A-8	Transverse Section of Cask Body	191
5-A-9,10,11	Drop Results	192-4
5-B-1-5	Photographs of Half Scale Mode Drop Tests	204-6
5-C-1-12	Photographs of Half Scale Model Fire Test	242-7
5-C-13	Computational Nodes	248
5-C-14-19	Calculated Full Scale Thermal Behavior	249-54
5-C-20	Calculated Thermal Behavior of Model	255
5-C-21	Test Duration vs. Fire Thermocouple Readings	256
5-C-22	Full Scale Model Section	257
DWG 9085-55	Half Scale Model	258
5-D-1	Thermal Model During Open Fire Tests	264
5-D-2	Condition After Fire Test	264
5-D-3	Fire Test of a TN9 Model-Records of Temperature	265
5-E1-2-3 q	Trunnion Stress	265x
5-E-4-54-6	Trunnion Stress	265y
5-E-7	Trunnion Stress	265z
7-C-1	TN8 Section	282a
7-D-1	TN9 Packaging-Configuration for Criticality Calculation	290a
7-E-1	TN-8/8L Model for Criticality Evaluation	290f
8-H-1	Trailer Loading/Unloading Operations	328
8-H-2	Protective Skirt Installation	329
8-H-3	VDS in Vent Mode	330
8-H-4	CDS in Cask Filling/Cooldown Mode	331
8-H-5	Loaded Cask in Draining Mode	332
8-H-6	Connector "C"	333
8-H-7	Skirt Fill System	334
8-H-8	Lid and Cover Bolt Tightening Sequence	335
8-H-9	VDS in Lid Tightness Testing Mode	336

8-H-10	VDS in "A" and "B" Opening Leaktightness Testing Mode	337
8-H-11	VDS in "C" Opening Leaktightness Testing Mode	338
8-H-12	Connector "B"	338a
8-H-13	VDS in Vacuum Drying Mode	338b
8-H-14	DELETED	338c
8-H-15	DELETED	338d
8-H-16	DELETED	338e
8-H-17	VDS in Backfill Mode	338f
DWG 9317-01	TN8 Packaging	353
DWG 9317-03	TN9 Packaging	354
DWG 9317-138	TN8L Packaging	355
DWG 9040-500-1	Configuration X Lid, Top View	356
DWG 9040-500-2	Configuration X Lid, Sectional Views	357
DWG 9040-500-3	Configuration X Lid, Parts List	358

- CHAPTER V -

CONFORMITY UNDER REGULATORY TEST CONDITIONS

In this chapter, we analyze the behavior of the packages (TN8 and TN9) under type B test conditions, as defined in Chapter VII of the IAEA Regulations.

1. TESTS COMMON TO TYPE A AND B PACKAGINGS

1.1. Water spray (§ 711)

This test does not affect these packages.

1.2. 0.3 meter free drop preceded by corner drop(*) (§ 712)

This test is far less severe than the 9 meter drop which is analyzed later.

The repeated drop tests performed on the 1/4 and 1/2 scale models of the TN9 packaging show that these tests do not reduce shielding of the contents or affect the leaktightness of containment vessel, or reduce substantially the heat dissipation to ambient air which relies upon natural convection through cooling fins protected against shocks by the extremity drums.

The damage caused by the 0.3 m or one foot drop would be similar to those observed with 9 m drop but reduced in extent.

(*) For compliance with 10 CFR 71 (Appendix A-6 and 7), this test is to be replaced by a one foot drop not preceded by a corner drop because the package weight exceeds 30,000 lbs and it is not fissile class II.

- An horizontal drop would cause a slight compression to the extremity drums and covers without damage to the fusibles which are protected by their recessed position at trunnion root.
- A vertical drop upon an extremity cover would cause its deformation without damage to other packaging constituents. Nevertheless, because of instability ot that vertical position upon a cover and possible subsequent fall to a horizontal position, we consider it is potentially the most damaging orientation.

We can predict deformations and decelerations corresponding to this case by referring to the results of the 1/4 scale model tests.

1st Phase : <u>Vertical drop on extremity cover</u>

We calculate the cover deformation and deceleration as follows :

- drop energy : $305 \times 3.6 \times 10^4 = 1.098 \times 10^7$ daN x mm
- cover surface : 2.2 m^2
- crushing resistance of balsa wood in fiber direction: 0.7 hb *
- force necessary to start cover crushing : 1.54×10^6 daN
- cover deformation : $\frac{1.098 \times 10^7}{1.54 \times 10^6} = 7$ mm
- deceleration : $\frac{305}{7} = 44$ g

We may assume that damages concern only the impact region as (cover) for such a low impact velocity (2.43 m/s) most of the package components may absorb cinetic energy without exceeding yield strength. In particular, the cinetic energy of lid and contents may be absorbe by the lid fixing screws without exceeding yield strength.

One reaches similar conclusions as concerns all orifices connected to the package cavity and the fusible screws connected to the compartment filled with wet cement.

(*) Refer to [38].

2nd phase : Fall to horizontal position

The vertical displacement of the package center of gravity corresponding to this fall is :

For TN 8	2.75 - 0.85 = 1.9 m
For TN 9	2.87 - 0.85 = 2.02 m.

For both packages, the fall energy is about the same because the weight difference is compensated by the fall height difference.
This energy is absorbed by deformation of the drum which was at the upper extremity before the drop. With reference to drop # 6 of the 1/4 scale model, (fig. 5.A.10), we can predict the present deformation of the drum.

$$\frac{12 + 29}{2} \times 2 \times 4 \times \frac{2.02}{9} = 37 \text{ mm}$$

The deceleration is : $\frac{2020}{37} \times 2 = 110$ g

which reflects the fact that the drum moves through twice the distance of the center of gravity during the fall.

As the deformation of the drum is limited to 37 mm, only a few cooling fins risk being bent and would have no potential influence upon changing the cooling rate of the package. Similarly, the fusibles and their connections to the cement compartment do not risk damage because of their recesses location at drum surface as well as the mechanical protection offered by the trunnions.

1.3. Compression (§ 713)

In Annex B to Chapter III, the stresses caused in the package by a uniformly shared load equal to five times the package weight were calculated. Resulting stresses are very small and do not affect the shielding efficiency or the leaktightness.

1.4. Penetration (§ 714)

This test obviously will not damage the package regardless of impact point as all feasible points of damage are protected by the shock absorbing covers.

2. TESTS SPECIFIC TO TYPE B PACKAGINGS

2.1. The TN8 and TN9 packaging designs incorporate the results of many studies which we have performed for about ten years concerning the specific problems facing the designers of type B packagings.

The objective of these studies was to find some simple and economical technology to solve these problems. Special emphasis was placed in the area of satisfying the regulatory requirements under accidental conditions.

Therefore, acting either alone or in cooperation with other organizations we:

- performed some drop and fire tests on various packaging designs
- developed technology to improve resistance to drops and fire
- established or checked theoretical and experimental methods of calculation to predict the behavior of packagings under regulatory accidental conditions.

Simultaneously, we collected and analyzed a pertinent theoretical and experimental bibliography especially concerning use of scale models to study packaging behavior [36].

An important part of our findings was published in reference [38].

In case of steel encased lead, we concluded that the following features are desirable:

- placing a veil of thermal insulation between the lead and the packaging outer shell. Cement is a particularly interesting insulating material because, although it acts as a thermal absorber avoiding the lead melting under accidental fire conditions, it does not affect the transmission of heat from the center of the package to the surface. Additionally, cement is economical and easy to use;
- providing shock absorbing covers at the packaging extremities.

Under regulatory test conditions, such features permit:

- absorption of the kinetic energy by deformation of subsidiary devices which have no functions in containment and shielding;
- reduction of lead settling in case of a tall packaging;
- reduction of damage to contents and of the stresses in the lid screws by a lower deceleration rate
- protection of the gaskets from high temperatures
- protection of the piping orifices which can easily be located under the shock absorbing covers.

As indicated in the detailed description of Chapter 11, those features were used in the TN8 and TN9 packaging designs. In order to verify the specific application of these features in the case of TN8 and TN9 (shock-absorbers made of balsa wood, cavity length, tubular trunnions, copper fins protruding from a resin layer, etc.), we chose to rely as far as possible on drop and fire tests on scale models, and to limit calculations to the analysis of design features introduced subsequently to test completion (recessed trunnions and lateral drain orifice). These calculations which concern the evaluation of the packages in drop test conditions are developped in the annex E to the present chapter.

2. 2. Principles of Model testing for predicting damage caused by the regulatory drop tests

Scale model testing is a method attractive for predicting the behavior of large packages during a drop, in particular when it is provided with shock absorbing structures, the deformation of which is difficult to evaluate by calculation.

It is based upon a theoretical analysis confirmed by an experimental work published in (36). This reference shows that similar lead models dropped from the same height will exhibit permanent deformations scaled as the models. This theory was also verified for complex models such as lead/steel containers or thick walled steel packages provided with aluminum shock absorbers at the extremities (38).

The general method to demonstrate validity of the model testing principle is to test a minimum of 2 models scaled in a geometric progression.

(for instance, 1/4 and 1/2 models.) The scaling factor between the actual full scale model and larger of the tested models is the same as between both tested models.

Most experimental work concerning model testing does not include acceleration measurements, but theory indicates that it varies according to the reciprocal of the scaling ratio.

It is obvious that the larger the model, the more convenient it is to include more design details. Therefore we decided to test a model at scale 1/2, the maximum reasonable considering the delay of fabrication and capacity of the testing facilities.

In addition, as we intended to have the main features of the 1/2 scale model as close as possible to that of the final design, we used a rather simplified 1/4 scale model which was easy to replace if necessary after testing. In fact, the first 1/4 scale model performed rather well and it was not necessary to significantly modify the design before proceeding to the more important 1/2 scale testing.

The characteristics of scale models used and the tests to which they were subjected are indicated in the following table:

SCALE MODEL					TESTS		
			Weight (kg)		Drops		Fire
Design	Scale	Ref. Dwg.	Total	Contents	Height	Nr.	
TN9	0.25	9085-44	530	41	9 m. 1 m/target 20 m. (**)	5 1 3	
TN9	0.5	9085-55	4 300	318	30' 40"/target 20 m. (*)	3 2 3	duration: about 15 min.
TN9	1	9085-69	2 000				duration: about 30 min.

* This test is not required by the Regulations but is shows that these packaging designs can withstand more severe drops than required.

As can be seen, the previous tests concern only the TN9 design. We can deduce from these tests conclusions conterning TN8 as well as TN9 designs because:

- The TN9 models survived repeated tests with a large margin of safety, thus we may assume that a slightly different design would also survive.
- The TN8 design is more compact and has a greater thermal inertia, therefore it would survive the same tests in better condition than the TN9 models.
- The two designs differ by less than 5% in weight, thus their behavior with regard to the 1 meter punch test may be regarded as similar.

2.3. DESCRIPTION OF THE MODELS AND RESULTS OF DROP TESTS (*)

2.3.1. Quarter scale model

The 0.25 scale model which was used to check the efficiency of the shock absorbers and the other characteristics of the TN9 packaging design was similar to the full scale packaging with some minor simplifications concerning mainly parts that do not contribute to structural strength (no fins, no resin, no cement veil, only one drain pipe, circular section of cavity, different type of lid gasket). In addition, carbon steel was used instead of stainless steel. This substitution is conservative since the properties of stainless steel are greater than carbon steel, and if the carbon steel model passed the tests, certainly the stainless steel model would have also.

One simplification which may have affected structural strength concerned the detail of radial reinforcements of the extremity drums which were not welded to the outer shell.

2.3.2. Half - Scale Model

The construction of this model reflected advancements made in the design since the testing of the 1/4 scale model. The 1/2 scale model reproduced most of the design details and also represented the fabrication to be used for the final design. All screws, semi-products and weldings were carefully scaled to represent as closely as possible those to be used in the full scale packaging.

(*) See also Annexes A and B

Differences from the full scale model include:

- Use of mild steel for external surfaces.
- Shape of the outer shell circular instead of polygonal with rounded angles.
- Copper fins replaced by long radial copper strips of same weight. The fact that twisted fins were replaced by parallel radial strips is very conservative when considering the retention of resin.
- Number of pipings to cavity reduced to 3 at critical locations and quick connections replaced by plugs.
- Truncated conical shape of lead shielding at lid extremity (eliminated in full scale to prevent gamma ray streaming).
- The external surface of lead is not stepped.
- The reinforcing places of the shock absorbing covers are made of carbon steel instead of stainless steel.

2.3.3. Drop Results

Both models survived the repeated drops without shielding reduction, loss of leaktightness or visible deformation of cavity even after the models were cross-sectioned for inspection.

The 0.25 scale model was drop-tested at ambient temperature (18°C) and the 1/2 scale model was preheated (80°C) prior to the first drop, but the results of the first drop in each series of tests were remarkably similar.

- For comparison of shock absorbing covers this result is important because after each drop in the 1/4 scale model tests the front cover was submerged in water to test for lid leakage whereas this was not done for the 1/2 scale model.

Because of the introduction of water into the cover, the results of the damage to the covers in the case of the 1/4 scale model for succeeding drops cannot be as closely correlated as in the 1/2 scale model.

Since the prime function of these tests was to subject the models to severe conditions and verify that they remained leak tight, close measurement of the extent of deformation (which would have been time consuming and expensive) was not concentrated upon. Emphasis was placed on completing all the planned drops within the time allowed to us at the testing facility.

- This result is also interesting because from 18°C to 80°C the ultimate strength of lead and its creep resistance are altered approximately the same amount as from 80°C to 144°C (maximum average temperature of lead during transport (*) as shown in the following table.

Temperature of lead (chemical lead)	Ultimate strength hb	Stress necessary to cause creep rate of 0.1% per year b
18°C	1.35	14
80°C	0.8	10
144°C	0.5	5.7

(*) See annex E to chapter IV

Therefore, we can consider that the deformations which the TN8 and TN9 packaging designs would suffer, at their temperature of utilization, are similar to those noticed on the scale models. Deceleration rates were measured by decelerometers and confirmed by a few measurements of deformations in the case of the 1/2 scale model.

For instance, consider drop No. 2 (vertical drop, on cover) of the half scale model.

Measurements:

model weight: 4 300 kg

initial thickness of balsa: 175 mm

final thickness of balsa: 89 mm - 2 x 2 mm = 85 mm

impact surface area (*) 0.4 to 0.45 m^2

maximum deceleration: 180 g

This decleration might be predicted by the following calculation:

compressive strain: $\frac{175 - 85}{175} = 0.515$

corresponding dynamic stress (38) P = 185 b.

static stress: $0.95\ b < p < 1.1\ b.$

max. deceleration: $D = \frac{P}{p}$

$168\ g \leqslant D \leqslant 195\ g$

(*) Taking into account drop No. 1 which compressed part of cover.

We see that the deceleration measured is within the range foreseen by calculation, taking into account the uncertainties in the estimate of the impact surface area.

As the regulations stipulate that the drop orientation and the impact point on target must cause maximum damage to the packaging, we carefully considered our choices to ensure compliance. It seemed that the most unfavorable 9m-drop orientation corresponded to a slight inclination which would position the center of gravity directly over the intended impact point. This is the orientation chosen to drop No. 1 (for both scale models). In both cases we also performed a vertical drop on the lid cover and a horizontal drop on the trunnions that gave rather similar results.

Two additional 9m orientations were adopted for the 0.25 scale model and both models were submitted to 20 meter drops. The half scale model covers which were cut apart for examination after the first series of tests were replaced prior to the series of 20 meter drop tests. In conclusion, we can assert that no 9 meter drop could cause any damage to the TN8 and TN9 packaging designs other than that noticed on the scale models.

Concerning punch tests, as preliminary studies showed that a particularly unfavorable orientation of drop on target is a vertical one which makes the target axis correspond with the packaging axis,

we reinforced the covers with stiffener stainless steel plates, the thickness of which was calculated to be sufficient to prevent damage to the piping orifices. The punch tests confirmed that the covers are not totally pierced and that leaktightness of the packaging is maintained. For a horizontal orientation, the punch did not damage the outer shell, nor cause any bending. As the sizes of the punches were scaled to agree with the tested models, these results demonstrate that the actual packaging would satisfactorily withstand the regulatory punch test.

These drop tests demonstrate that the contents would not damage the packagings as the scale models contained steel or lead weights which represented the TN9 contents.

In an attempt to check the condition of fuel pins after repeated drops, standard sized Zircalloy clad fuel pins were placed in the cavity of the 0.25 scale model without any packing. Obviously, these pins were not irradiated and therefore not stressed due to fission gas pressure.

It is interesting to note that these pins suffered no damage during the drops even though they were exposed to a deceleration four times that expected in the case of the actual packaging submitted to similar drops.

Measurements of the local deformations caused by the drop was not included in our testing program because such measurements require too much time and skill to be reliable and difficult to interpret as successive drops interfere with each other.

We preferred to take photos and movies (normal and high speed of 1/2 scale model). This was more efficient because the time allocated to tests was restricted and repeated drops seemed more useful than plain measurements that do not contribute directly to the evaluation of model behavior with respect to maintenance of shielding and leaktightness (main objectives of tests.)

We nevertheless measured the order of magnitude of deformations in several instances. In addition, for the 1/2 scale model we measured the decelerations as already stated.

In the following table we listed the main measurements and values for the full scale model extrapolated by multiplying the actual deformation measurements by the reciprocal of the scaling factor and multiplying the deceleration measurements by the scaling factor. For instance, a deceleration of 20 g measured with 1/2 scale model leads to a deceleration of 20 x 1/2 = 10 g for full scale and a deformation of 20 mm measured on the 1/4 scale model leads to a deformation of 20 x 4 = 80 mm for the full scale model.

Drop Orientation	Permanent Deformation and/or Deceleration(**)		
	Measured		Extrapolated
9 meter drop/ flat surface	1/4 scale model	1/2 scale model	Full scale model
- slightly inclined from vertical		160 g	80 g
- vertical upon lid cover (already damaged by previous drop)	(10mm)**	86 mm 180 g	172 mm 90 g
- horizontal upon trunnions (xxxxx)		150-180 g	75-90 g
- vertical upon undamaged cover	20 mm		80 mm (155 g)****
- horizontally upon drums	$\frac{12 + 29}{2}$ = 20mm		80 mm (155 g)
1 meter drop/punch			
- vertical upon rear cover		170 mm 20-60 g	340 mm 10-30 g
- horizontal upon finned region		20 g	10 g
- vertical upon lid cover (already damaged)	(90 mm)***		(360mm)

* Deformations are expressed in mm and acceleration taking the gravity as a unit (g). Note that deformations and accelerations are not corrected for accumulative effect of preceding drops.

** Balsa wood is wet.

*** Cover was reinforced as a consequence of this result.

**** Deduced from deformation measurement.

xxxxx Trunnion design was modified subsequently to the tests, but that modification would not affect the deceleration peak (refer to Annex E to this chapter).

3. Fire Test

3.1 Behavior of 0.5 scale model

After the drop tests previously mentioned, the 0.5 scale model was submitted to a fire test to check the ability of the packaging to survive the regulatory fire test conditions.

Annex C to the present chapter describes and analyzes the test performed and shows that:

- the shielding integrity and containment vessel leaktightness were maintained.
- the results can be applied to full scale packagings when submitted to a regulatory 30 minute fire test at 800°C.

At the end of the fire test, the 0.5 scale model was damaged to such a small extent that we were able to submit it to an additional series of seven drops which also did not affect its leaktightness and shielding.

This fire test pointed out that the resin shielding acts as a thermal insulation during the fire but may continue to burn after the fire is extinguished. This is due to the polyethylene content of the resin. The rate of post-combustion observed with the 0.5 scale model was rather low and did not seem to be contributing to the heating; thus, due to a time constraint. the test was concluded without waiting for self-extinction of the resin fire. In order to evaluate the consequences of a post-combustion period and eliminate any risk of error due to scaling, we decided to perform another fire test using the full scale slice of the packaging.

3.2. Calculation of fire test temperatures

In the early design period, these temperatures were determined by a graphical method [38].

We assumed:

- total power dissipated by the package 24.5 kW
- linear power 6.05 kW/m
- ambient temperature before fire
- thickness of the cement veil 6 mm
- fire conditions as specified in the regulations (Annex IV - I-4.3.2.)

The following table lists the results:

Time (since beginning of fire (minutes))	Temperatures (°C)					
	t_o ambient	t_1 fins	t_2 outer steel shell	t_3 external lead surface	t_4 internal lead surface	t_5 cavity
0	38	72	91	92	106	122
15	800	580	195	188	122	124
30	800	670	308	298	157	127
45	38	190	282	280	176	142

Maximum outer shell temperature (t_3 = 322°C) is attained 35 minutes after the beginning of the fire.

Annex C includes also a computer calculation which points out the influences of the thickness of the cement veil and of decay heat.

As these conditions do not consider post-combustion of resin, they are not sufficient to complete the entire fire test analysis but they were utilized for correcting the results obtained from the fire test described below and to take into account possible change of initial thermal equilibrium (ambient temperature, decay heat, solar load and cement veil thickness).

3.3 Behavior of full scale slice of TN 9 model and utilization of results for predicting temperatures of TN 8 and TN 9 under fire conditions

The full scale packaging slice already described in Annex A to Chapter IV was submitted to a regulatory open fire test § 723 of Ref (45). This test is described in Annex D of the present chapter. The model exhibited good resistance to the combined effects of internal heating and exposure to fire.

The results of this test may be used for predicting the behavior of the TN8 and TN9 models under the regulatory fire test conditions after adequate corrections.

3.3.1. Initial thermal equilibrium

The ambient conditions met during the fire test differed from those specified by U. S. regulations:

- air temperature was 17°C instead of 54.5°C (130°F)
- wind speed was 2-3 m/s instead of zero (still air)
- solar load was negligible instead of equivalent to 2420 kcal/h for the full package.

3.3.2. Information resulting from fire test

The temperature records of the test (fig.5.D.3) show that the outer shell temperature increases rather quickly during the gasoline fire period (0 - 30 min), then is practically stabilized during a 150 min period corresponding to resin combustion (30 min - 100 min) before decreasing quickly.

As shown on fig. 5.1. :

- during the fire period (A - B),

  t_3 (outer shell temperature) varied by 223°C from 27°C to 250°C

  t_4 (external lead temperature) varied from 46°C to 100°C

  t_{3-4} (difference between t_3 and t_4) varied from -19°C to 150°C

- during the resin combustion period (B-C)

  t_3 practically remained at 320°C (average of actual temperatures)

  t_4 varied from 100°C to 228°C

  t_{3-4} varied from 220°C to 92°C

For predicting the behavior of TN8 and TN9 packages, it seems reasonable to admit (as observed with tested model) that the outer shell temperature varies by 223°C during period (A - B), then remains at 320°C during period (B - C).

In addition, the fire test results permit calculating the apparent conductivity (k) of the insulating veil between the outer shell and the lead during the period (B - C).

Let us consider a piece having a heat capacity (ΣMC) developing an internal heat load (Q) and isolated from a surrounding shell at constant temperature (t_3) by an insulating veil (thickness: e; surface : s; conductivity: k).

At any time (Θ), the temperature gradient (t_{4-3}) through the insulating veil is given by the equation:

$$(t_{4-3}) \times \frac{ks}{e} + Q = \left[(t_{4-3})_{\Theta=o} \times \frac{ks}{e} + Q\right] e^{-B\Theta}$$

$$\text{with } B = \frac{ks}{e\Sigma MC}$$

The following table gives the data necessary to solve above equation :

	Fire tested model of TN9	TN8	TN9
Q (kcal/h)	1550.	30,530	21,070
e (m)	0.01	0.005	0.005
s (m^2)	0.86	9.9	10
Σ MC (kcal/°C)	57.5	1022	961
S/e ΣMC	1.49	1.94	2.08

Remarks : 1 - Veil thickness chosen is a minimum, taking into account the fabrication tolerances.

2 — For the determination of the veil surface, we consider the length corresponding to reduced thickness (3.30 m for TN8 and 3.54 m for TN9)

3 - For determination of MC, we consider the weights of materials surrounded by cement (fuel excluded) :

Material	Specific heat (kcal/kg°C) [13]	Weights (kg)		
		Fire Tested Model	TN8	TN9
Steel	0.106	87	1200	1500
Lead	0.038	1270	20700	20700
Copper	0.092	0	300	170
Resin	1	0	50	50
B4C-Cu	0.124	0	250	

Considering the period B-C of the fire test, we have :

$\Theta = 2.5$ h

$(t_{4-3})_C = 92°C$

$(t_{4-3})_B = 220°C$

and equation page 181 (a) gives :

$$\frac{ks}{e} = 9.2 \qquad k = \frac{9.2 \times 0.01}{0.86} = 0.107 \text{ kcal/h.m}^2$$

Note : Such a low thermal conductivity seems to indicate the presence of gaseous gap.

3.3.3. Prediction of the external lead temperature (t_4) in fire conditions

(a) TN8 Package (see fig. 5.2.)

During period A-B, shell temperature (t_3) varies from :

$(t_3)_A = 114°C$ to $(t_3)_B = 114 + 223 = 337°C$

Referring to the corresponding variations measured during the fire test and introducing a correction for minimum cement thickness, heat capacity and heated surface, we find that temperature t_4 varies from :

$(t_4)_A = 114 + \frac{20}{2} = 124°C$ (cement veil 5 mm thick)

to $(t_4)_B = 124 + (100 - 46) \times \frac{1.94}{1.49} = 194°C$

During the period B-D, t_3 remains at 320°C.

At time B : $(t_{3-4})_B = 320 - 194 = 126°C$

Equation (page 181 a) gives t_{3-4} at time C :

$B\theta = 1.94 \times 0.107 \times 2.5 = 0.519$

$e^{-B\theta} = 0.595$

$(t_{3-4})_C = 17°C$

$(t_4)_C = 320 - 1.7 = 303°C$

b) <u>TN9 Package</u> (see fig. 5.3.)

During period A-B, the shell temperature varies from $(t_3)_A = 165.5°C$

$(t_3)_B = 105.5 + 233 \neq 329°C$

and external temperature of lead varies from :

$(t_4)_A = 105.5 + \frac{14,5}{2} = 113°C$ to

$(t_4)_B = 113 + (100 - 46) \times \frac{2.08}{1.49} = 188°C$

At the beginning of period B - C,

$(t_{3-4})_B = 320 - 188 = 132°C$

At time C,

$B\theta = 2.08 \times 0.107 \times 2.5 = 0.556$

$e^{-B\theta} = 0.573$

Equation (1) gives :

$(t_{3-4})_C = 32°C$

$(t_4)_C = 320 - 32 = 288°C$

3.3.4. <u>Maximum transient temperatures of different package constituents</u>

At time C, the heat received from ambiance decreased to 9 - 16% of the contents load. Therefore one may assume that the temperature repartition through lead became approximatively parabolic and that the temperature gradient does not exceed half its value in normal transport conditions (temperature repartition approximatively linear). For the determination of the maximum transient temperature of the fuel pins (t'm) we refer to formula in chapter IV. Results are given in the table at the end of this paragraph.

3.3.5. Equilibrium temperatures after the fire test

Fig. 5.D.3 gives the following temperatures measured at equilibrium for the fire tested model.

Temperature	Initial equilibrium	Final equilibrium
t_0	17	17
t_3	27	50
t_4	46	84
t_5	63	115
t_6	125	178

- The fin efficiency was reduced as a consequence of distortion, local melting and oxidation, but most of the burned resin remained in place.
- It seems reasonable to assume that this reduction did not exceed a factor of two.
- Dehydration of the cement caused the gradient (t_{5-3}) to vary from 36°C to 65°C (80% increase).
- Thermal gradient (t_{6-5}) did not vary.

These results and interpretations allow determination of the equilibrium temperatures of TN8 and TN9 packages after the fire conditions.

[For determination of fuel pin temperatures (tm), we refer to chapter IV.

3.3.6. Behavior of TN8 and TN9 models under fire conditions

3.3.6.1. Consequences of temperature changes

The calculated temperatures are given in the following table :

Location	Temperatures in normal transport conditions (°C)				Maximum transient temperatures (3)	
	Before fire (1)		After fire (2)			
	TN8	TN9	TN8	TN9	TN8	TN9
Outer shell (t_3)	114	106	175	160	320	320
External lead surface (t_4)	126-134	115-120	232	198	303	288
Internal lead surface (t_5)	154-162	132-137	260	215	317	297
Hottest compartment average (t_6)	164-172	286-291	268	369	427	451
Fuel pins (tm)	443-445	369-374	490	430	525	496

(1) Temperature values are subject to possible variations due to fabrication tolerances which cause differences in the thickness of the cement veil (5 to 10 mm).

(2) We consider only maximum thickness of cement veil (10 mm).

(3) We consider only minimum thickness of cement veil (5 mm).

Since the melting temperature of lead is 327°C, the packaging does not risk melting during or after the test.

The containment vessel remains leaktight because the silicone rubber gaskets withstand the temperatures reached during and after the test maximum 303°C for a short period and 232°C at equilibrium).

3.3.7 TN-8L Fire Accident

The fins provide the principal path for heat transfer from a fire into the packaging. The solid resin shielding acts as a thermal insulation during the fire. Since the TN-8L has a lesser number of fins, the total heat flow into the packaging will be less and all internal temperatures will be lower than those predicted for the TN-8.

3.3.8 TN-8 Fire Accident with Type "PP" Fuel

3.3.8.1 Maximum Transient Temperatures After Fire

From Chapter IV, t_3 = 67.4°C and t_4 = 69.1°C are the steady state temperatures with an ambient temperature of 54.5°C, an insolation heat load of 2.9 kw and a decay heat load of 3.0 kw. Let A be the time at the start of the fire test. Time B (30 minutes later) is when the fire is extinguished and the time C is 180 minutes after the start of the fire (150 minutes after the fire is extinguished).

Using the results of the fire test on the slice of the full scale model, we have

$$(t_3)_B - (t_3)_A = 223°C$$

For $(t_3)_A = 67.4°C$, $(t_3)_B = 223 + 67.4 = 290°C$

To be conservative for the fire conditions, the cement layer thickness is reduced to the minimum value of 0.005 m.

Therefore,

$$(t_4)_A = 67.4 + 69.1 - 67.4/2 = 68°C$$

The temperature $(t_4)_B$ in the TN-8 package is predicted from the results of the test model. A correction for the difference in heat capacity and heated surface area between the TN-8 package and the test model is made using the formula

$$(t_4)_B - (t_4)_A = [(t_4)_B - (t_4)_A]_{\text{test model}} \times (B'_{TN-8}/B'_{\text{test model}})]$$

where

$$[(t)_B - (t_4)_A]_{\text{test model}} = 100 - 46 = 54°C$$

$$B' = S/(e \quad M_i \; C_i)$$
$$B'_{\text{test model}} = 1.49 \text{ m°C/kcal}$$
$$B'_{TN-8} = 1.94 \text{m°C/kcal}$$

By substitution of these data into the formula above, $(t_4)_B$ can be calculated as

$$(t_4)_B = 70 + 68 = 138°C$$

As in the case of the test model, it is assumed that t_3 remains at 320°C during period B-C. At time B,

$$(t_{3-4})_B = (t_3)_B - (t_4)_B = 320 - 138 = 182°C$$

To determine the temperature gradient across the cement layer, the same equation which was used for the TN-8 package is employed. Namely,

$$(t_{4-3})_T \times \frac{ks}{e} + Q = [(t_{4-3})_{T=0} = 0 \times \frac{ks}{e} + Q] \times \exp(-BT)$$

At time T. the temperature gradient (t_{4-3}) through the cement layer is given by this equation where

$$B = \frac{k\,S}{e \sum M_i C_i}$$

Time O between events B and C is 180 - 30 = 150 minutes (2.5 hr). Additional data are as follows:

k = 0.107 kcal/hr.m.°C
Q = decay heat load = 2580 kcal/hr
S = surface area of cement layer = 9.9 m^2
B = B' x k = 1.94 x 0.107 = 0.208 hr^{-1}
exp(-BT) = exp (-0.208 x 2.5) = 0.595

ks/e = 0.107 x 9.9/0.005 = 212 kcal/hr°C

By substituting the appropriate values in Eq. 3.1. we get

$(t_{3-4})_C$ = 103°C

$(t_4)_C$ = 320 - 103 = 217°C

The calculations show that under fire accident conditions for the temperature of the outer shell at 320°C the maximum transient outer lead surface temperature (t_4) of the TN-8L package with 3 kw decay heat load is 217°C. This temperature is less than the corresponding value for the TN-8 packaging (303°C).

During the fire accident, the lead temperature increased by $(t_4)_C - (t_4)_A = 217 - 68 = 149°C$. Since the lead layer completely encloses the fuel assembly region, the average cavity gas temperature will not increase by more than the increase in lead temperature during the accident. Since the cavity gas temperature during normal transport conditions is 94°C, the maximum cavity gas temperature will not be more than 94 + 149 = 243°C for the TN-8 and TN-8L packages.

3.3.8.2 Equilibrium Temperatures After Fire

The TN-8L packaging temperatures at equilibrium after the fire can be deduced from the TN-8 packaging temperatures by applying the appropriate corrections to account for total heat load P, number fins N_f, and decay heat load per assembly Q. The TN-8 package will hav elower equilibrium temperatures than the TN-8L because the TN-8 has more fins than the TN-8L.

(a) Outer Shell Temperature, t_3

$$(t_3 - t_o)_{TN-8L} = (t_3 - t_o)_{TN-8} \times \frac{(N_f)_{TN-8}}{(N_f)_{TN-8L}} \times \frac{P_{TN-8L}}{P_{TN-8}}$$

Where

$(t_3 - t_o)_{TN-8}$ = temperature difference between the outer shell and ambient for the TN-8 package = 120.5°C

$(N_f)_{TN-8}$ = Number of fins on TN-8 package = 22,000

$(N_f)_{TN-8L}$ = Number of fins on TN-8L package = 15,800

P_{TN-8} = Total heat load (including solar heat) = 38.3kw

P_{TN-8L} = Total heat load (including solar heat) = 5.9kw

t_o = ambient temperature = 54.5°C

Therefore,

$$(t_3 - t_o)_{TN-8L} = 120.5 \times \frac{22,800}{15,800} \times \frac{5.9}{38.3} = 26.8°C$$

$$t_3 = 26.8 + 54.5 = 81.3°C$$

(b) External Lead Surface Temperature, t_4

$$(t_{4-3})_{TN-8L} = (t_4 - t_3)_{TN-8} \times \frac{Q_{TN-8L}}{Q_{TN-8}}$$

where

$(t_4 - t_3)_{TN-8}$ = temperature difference across cement layer for the TN-8 package = 38°C

Q_{TN-8L} = decay heat load for the TN-8L package = 1.0 kw/assy.

Q_{TN-8} = decay heat load for the TN-8 package = 11.84 kw/assy.

Therefore

$$(t_4 - t_3)_{TN-8L} = 38 \times \frac{1.0}{11.84} = 3.2°C$$

$$t_4 = 81.3 + 3.2 = 85°C$$

As the lead layer completely surrounds the fuel assembly region, the average cavity gas temperature will not increase by more than the increase in lead temperature at equilibrium after the fire accident. The lead temperature t_4 increased from 69.1°C to 85°C, i.e., by 16°C. The average cavity gas temperature during normal transport conditions was assessed as 94°C. Therefore, the cavity gas temperature at equilibrium after the fire accident will not be more than 94 + 16 = 110°C for the TN-8 and TN-8L packages.

The viton gasket has been conservatively assumed to be at a temperature equal to t_4, the external lead temperature. Hence the average gasket temperature is assumed to be 85°C at equilibrium after the fire accident.

3.3.8.3 Conclusions

The results of the thermal evaluation indicate that the temperature distribution in the TN-8 or TN-8L packages carrying three "PP" or "PP1" type fuel assemblies precooled for five years is much lower than that presented for the TN-8 carrying three "P" or "P1" assemblies.

The average cavity gas temperatures were estimated to be not higher than 243°C and 110°C in transient fire accident and post accident equilibrium conditions, respectively. These temperatures are much lower than the corresponding values, namely 450°C and 390°C respectively, reported for the TN-8 package with 150 day cooled fuel.

3.3.9 Consequences of Pressure Changes

(a) Peak Cavity Gas Pressure

The peak cavity gas pressure will occur at the maximum cavity gas temperature and when the cavity contains the maximum amount (mass) of gas. This could occur during a fire accident if all the fuel pins fail. The peak pressure is evaluated assuming this hypothetical accident occurs.

The maximum partial pressure of nitrogen is

$$P_N = t_{7max}\ V_6(T_1\ V_7) \times P$$

and the maximum partial pressure of free gas released by the fuel is

$$P_F = t_{7max}\ 3V_3/298\ V_7 \times P$$

where

P is the cavity pressure at equilibrium = lb (section 1.1.9)
t_{7max} is the maximum transient gas temperature, °K
t_1 is the equilibrium cavity gas temperature, °K
V_6 is the cavity free volume before the accident
= TN8 cavity volume - 3 x (assembly volume*)
V_7 is the cavity free volume after the accident

and V_3 is the free gas (NTP) per assembly

*Chapter III, Annex C

i) TN-8/TN-8L with Type "P" Fuel

$T = 573$ °K (Ch. IV, Section 6.0)
$T_{7max} = 723$ °K (Ch. IV, Section 6)
$V_3 = 0.112\ m^3$ (Ch. III, Annex C, Section 1.1.5)
$V_6 = 0.453\ m^3$ (Ch. III, Annex C, Section 1.1.7)
$V_7 = 0.461\ m^3$ (Ch. III, Annex C, Section 1.1.8)

$$P = P_N + P_F$$

$$= \frac{723}{573} \times \frac{0.453}{0.461} \times 1.0 + \frac{723}{298} \times \frac{3\ (0.112)}{0.461} \times 1.0$$

$$= 1.24 + 1.77\ b$$

$$= 3.0\ b$$

ii) TN-8/TN-8L with Type "PP" Fuel

Fuel data provided by vendors show that the assembly volume for "PP" fuel may be as large as 0.091 m^3. It also has been observed that these assemblies have larger "pin void" volumes. The combinatin of these two factors result in a small increase in peak cavity pressure during a hypothetical fire accident. This has been accounted for in the calculation of maximum pressure for various combinations of residual heat and free gas volume per assembly. The results are presented in TAble 5.1. The maximum cavity pressure is 3.7 bar absolute.

The table shows that fuel assemblies with more free gas per assembly may be transported in the TN-8L cask if the decay heat load is lower. This may be achieved by stipulating a longer cooling period after discharge for spent fuel with high free gas content. Correspondingly, assemblies having lower volumes of free gas per assembly and higher decay heat loads may also be transported.

c) Risks associated with pressure increase

Above calculated pressures remain far below the testing pressure (11 b) and do not risk damaging the packaging or causing leakage.

4. Conclusions

The results of drop and fire tests on packaging models illustrate that all designs comply with regulatory requirements concerning type A and B packagings.

The consequences of regulatory tests are:

- temperature increase of packaging and contents: this increase does not damage the packaging or modify the physical or chemical form of the contents nor does it appreciably change the primary coolant pressure (*).

- deformations: they are limited to externals and do not affect the cavity. The integrity of the containment vessel and the gamma shielding is insured.

- loss of the main neutron shielding as a result of resin combustion: it is shown in Annex A to Chapter III that the regulatory dose rate limits (1000 mrem/h at 1 meter from the package surface) are not exceeded

---

(*) The flattening of the fuel pin array and the rupture of fuel pin cladding may occur as a consequence of the drops. They do not risk increasing the package reactivity (see Chapter VII) nor do they cause significant pressure change inside the package cavity.

TABLE 5.1

DEPENDENCE OF MAXIMUM FREE GAS CONTENT ON DECAY HEAT LOAD, TN-8 and TN-8L

Parameters	Decay Heat Load Per Assembly (kw) 0.5	1.0	3.0	5.0	7.0	9.0
Average temp. at contact surface between outer shell and cement layer, t_3°C	64.1	67.4	80.7	94.1	107.4	120.6
Average temp. at contact surface between cement layer and lead, t_4 °C	64.9	69.1	85.8	102.5	119.2	135.8
Average compartment wall temperature, t_6°C	66.6	72.4	95.6	118.8	142.0	165.2
Maximum Fuel Pin Temp., t_m°C	89.6	116.4	208.6	282.8	344.0	395.2
Cavity gas temperature (normal transport condition), t_1°C	78.1	94.4	152.1	200.8	243.0	280.2
Max. cavity gas temperature (fire accident), t_{7max}°C	230.8	243.1	304.6	357.1	403.0	444.0
Max. free gas (NTP) per assembly, V_3 m^3 (1)	0.186	0.181	0.161	0.147	0.136	0.128
Maximum Pressure (bar)	3.69	3.66	3.60	3.56	3.53	3.51

Notes: (1) It is assumed that the cavity gas pressure at equilibrium = 1.0 b, and the cavity temperature at closure = $t_c = (t_6 + t_m)/2$

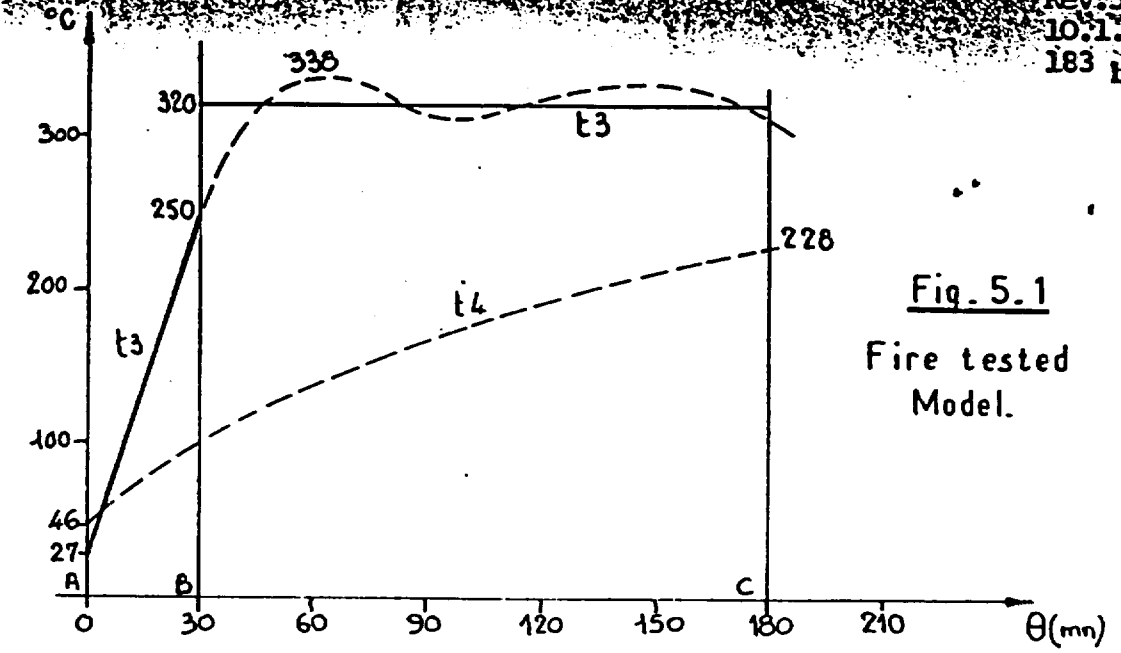

Fig. 5.1

Fire tested Model.

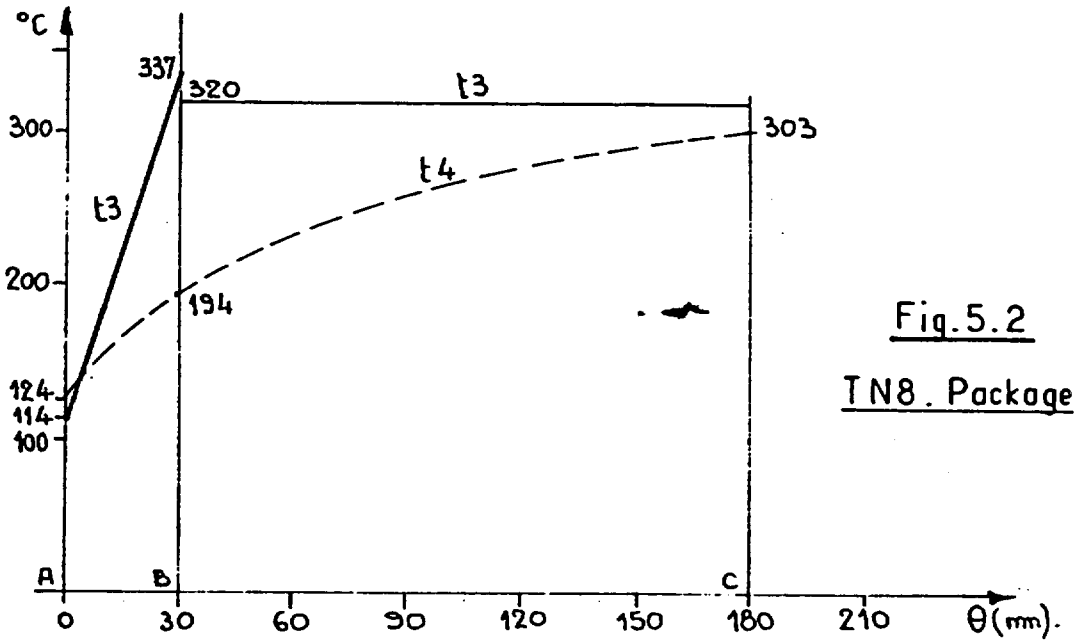

Fig. 5.2

TN8. Package

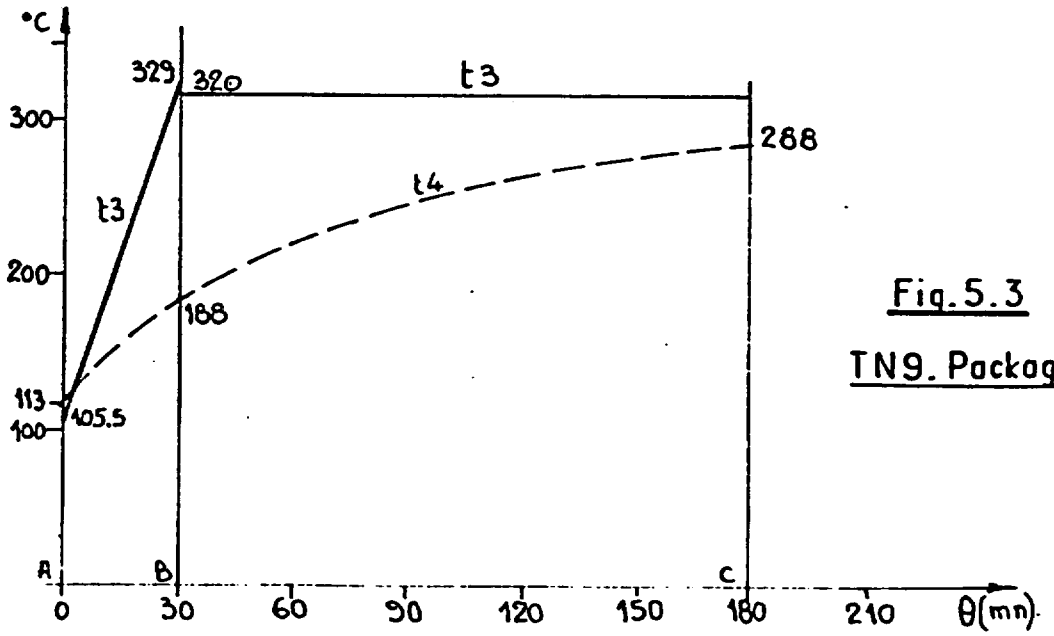

Fig. 5.3

TN9. Package

N° 5 (7.62. le 7.1.76.

- ANNEX A TO CHAPTER V -

DROP TESTS OF TN9 CASK, QUARTER SCALE MODEL

May 13, 1971

SUMMARY

A 1/4 scale model of the packaging was subjected to a total of 9 drops up to 20m onto different targets. The model remained leaktight. Deformation of the containment was very limited.

1. INTRODUCTION

The purpose of the drop tests was to collect the following information:

- Efficiency of shock absorbers
- Comparison of results with half scale model
- Condition after drops (20m) exceeding regulatory requirements
- Condition of Zircalloy-clad fuel pins after several drops

2. DESCRIPTION OF THE PACKAGE (Fig. 5-A-1)

Reference drawing TN 9085-44

Materials:

- carbon steel
- lead
- Balsa wood

Contents:

- 40 Kg lead cylinder maintained by two wooden spacers
- 3 fuel pins, each 13 mm diameter, 345 mm long (type FR-2) - without packing

The model was 1443 mm long and 429 mm in diameter including shock absorbers. It simulated the main features of the TN9 design as far as we suspected they would influence its behavior under the conditions of the drop tests (weight; length; diameter of extremities; thickness of Balsa and steel parts; number, length, core diameter and material of screws).

In order to facilitate manufacturing, the following simplifications were adopted:

- circular shape of inner and outer shells
- deletion of resin, copper fins and cement veil
- one drain
- stainless steel replaced by carbon steel

The lid did not have o-ring gaskets but was simply tightened by silicone rubber. An initial leaktightness test at 3 bar was conducted.

Weight breakdown is given below:

- packaging body and lid	475 Kg
- 2 shock absorbers	14 Kg
- contents	41 Kg
Total	530 Kg

3. FUEL ROD CHARACTERISTICS

Cladding: Zircalloy 2

O.D.: 13 mm

Wall thickness: 0.65 mm

Pellets: natural UO_2

Length: 345 mm

Plugs: WIG welded

No spacer spring

4. TEST FACILITY

The target was a 12 mm steel plate on a 35 T block of concrete set in soil.

The model was lifted by a mobile crane and released by a mechanical system.

Tightness was tested by pressurizing the model with air and submerging the lid region in water. Absence of gas bubbles indicated tightness.

A steel bar 35 mm in diameter and 100 mm long rigidly mounted perpendicularly to the steel plate was used in the punch test.

5. DROP TESTS

See results on following pages.

6. INSPECTION OF THE MODEL AFTER THE TESTS

6.1. Shock absorbers

All the screws of both shock absorbers were still in place and could easily be removed after removal of balsa wood.

6.2. Pressure tests

After drop No. 9, a soap bubble test with 1.5 bar air pressure was performed. The container was tight. After removal of the contents the lid was fixed again using liquid silicone as gasket material. The container was leaktight when tested with 2.8 bar air pressure.

6.3. Dimensional changes (Fig. 5-A-5)

The lid and its housing were checked for dimensional changes:

- Out-of-roundness was within 0.1 - 0.2 mm which is probably the tolerance as manufactured.
- The transition from the lid housing (150 mm Ø) to the cavity (120 mm Ø) was deformed slightly (it is not known if it was that way before the tests).
- The lid was depressed by the punch about 10 mm. No bending of the flange was noticed.
- The lower end was cut into pieces. From fig. 5-A-6 it can be seen that the trunnion did not dent the outer shell but was compressed like a bellows. Though the shock absorber was heavily deformed, the outer shell, the lead shielding and the fuel housing were not affected. (See fig. 5-A-7 and 5-A-8)

6.4. Condition of Contents

The lead cylinder was squeezed in the last third of the cavity and could not be removed. Its wooden spacers were partly crushed. One of the 3 fuel pins was slightly bent; all of them remained leaktight. Radiography showed that the pellets were not crushed and that their original form remained. In fact, one cannot find a difference between the x-ray pictures of a pin before and after the tests.

7. DISCUSSION

Performance of the model was excellent except for the puncture test. Puncture close to the lid flange might have caused loss of tightness. As it was observed that penetration of the punch was almost the same as its length, we concluded that the reinforcing plates of the covers should be made of stainless steel of the same thickness or thicker, if made of carbon steel.

The method used for testing the lid tightness (immersion of the lid region) may have changed the results of drops upon the lid cover (except for the first drop) because it caused the balsa wood to be impregnated by water. When impregnated by water, the balsa loses part of its compressibility and increases its elastic range.

FIGURE WITHHELD UNDER 10 CFR 2.390

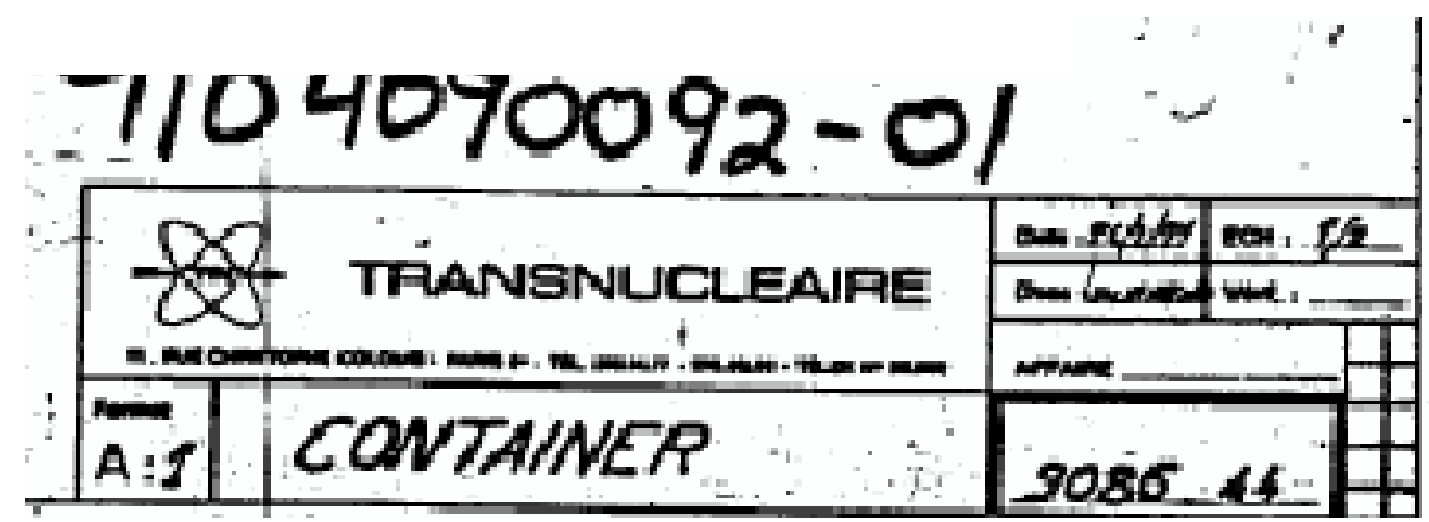

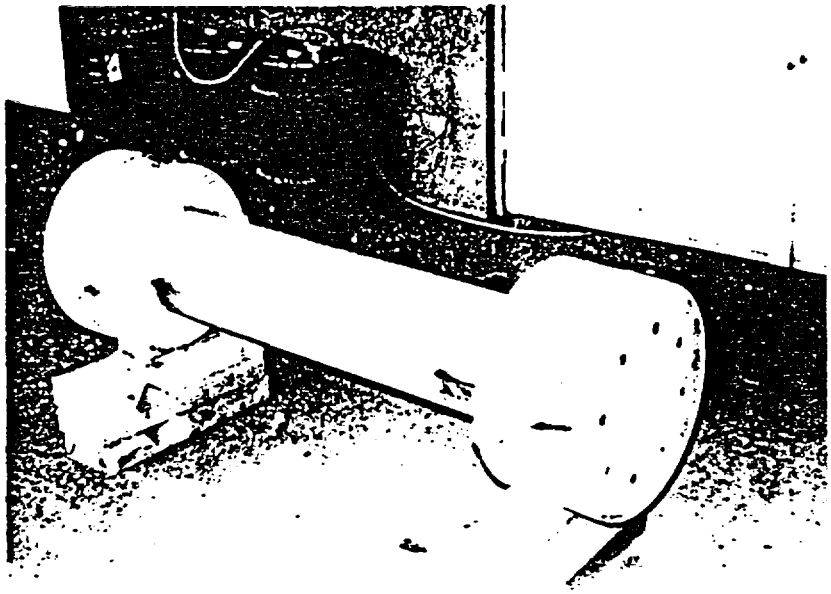

Fig. 5.A.1 – *1/4 scale model of TN9 before tests*

Fig. 5.A.2 – *1/4 scale model of TN9 - Deformations of trunnion and front cover after 2nd 9 meters drop.*

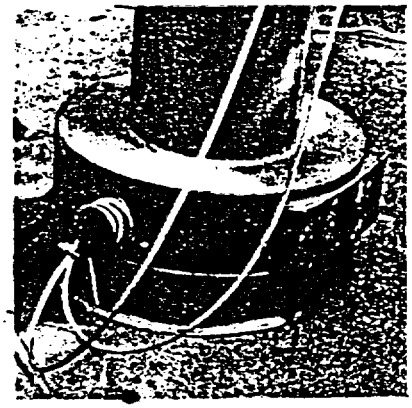

Fig. 5.A.3 – *1/4 scale model of TN9 - Condition after 9 meters drop onto rear cover.*

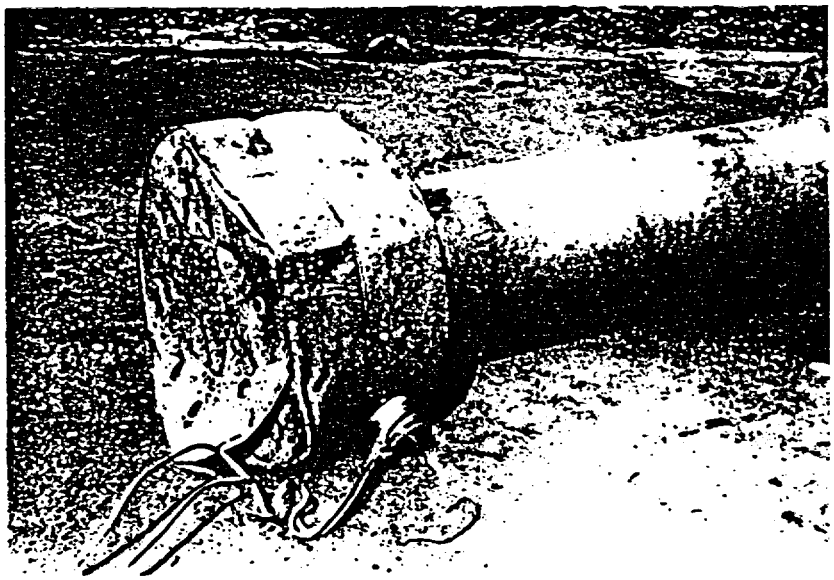

Fig. 5.A.4 – *1/4 scale model of TN9 - Condition after 9 th drop (20 meters)*

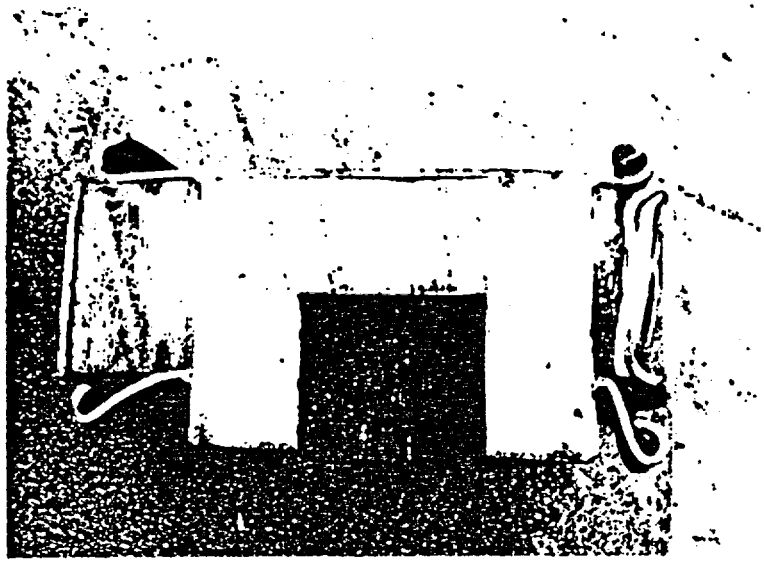

Fig. 5.A.7 – *1/4 scale model of TN9 - Longitudinal section through cask body (bottom)*

Fig. 5.A.6 – *1/4 scale model of TN9 - Section through cask bottom showing collapsed trunnion.*

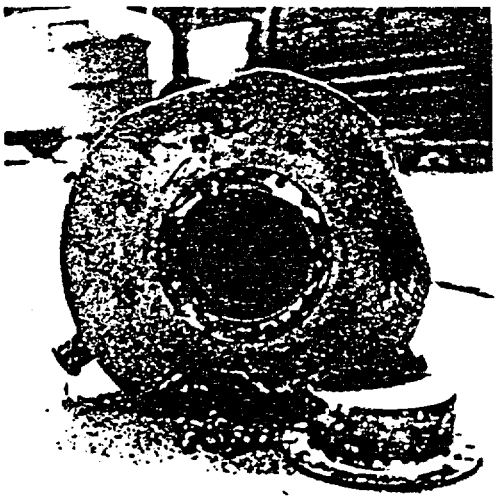

Fig. 5.A.5 – *1/4 scale model of TN9 - Condition of lid and lid lodgment after 9 th drop*

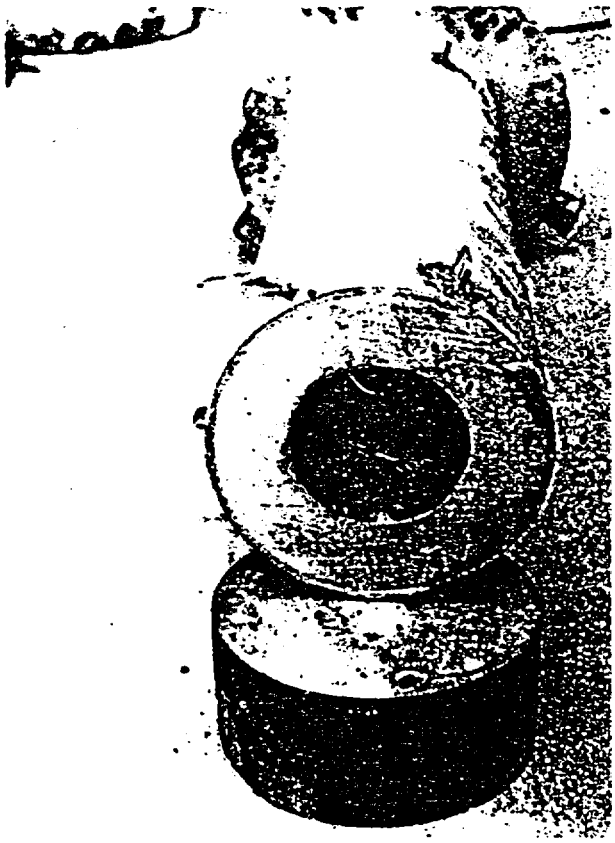

Fig. 5.A.8 – *1/4 scale model of TN9 - Transversal section of cask body.*

DROP NR.	DROP	ORIENTATION OF MODEL	RESULTS OF DROP	FIG. Ref.
1	9 m	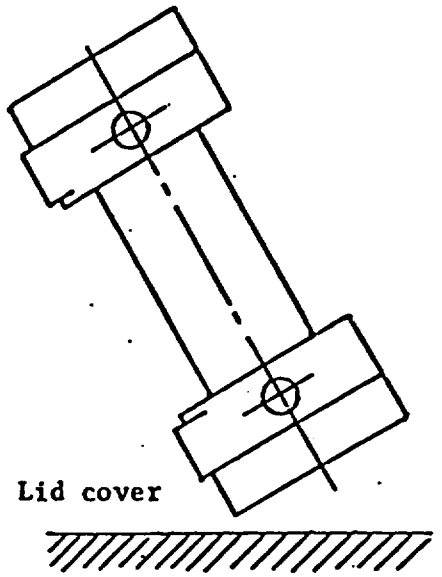	- cover evenly squeezed - cracks in welded rim of cover 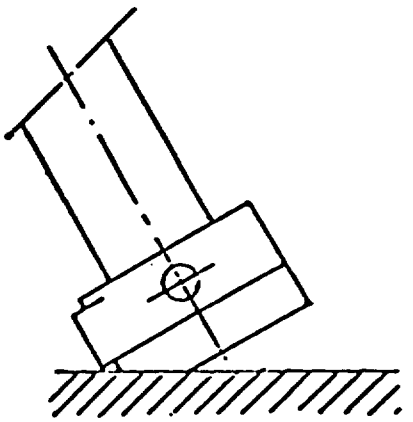	
2	9 m	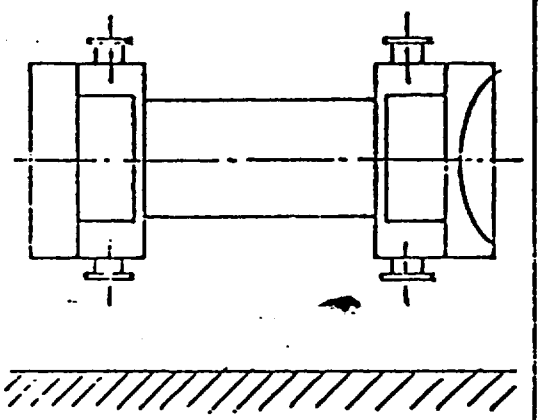	- trunnions disappeared into the model body - bubble test : tight (air pressure at 3,5 bar)	5.A.2
3	1 m onto punch	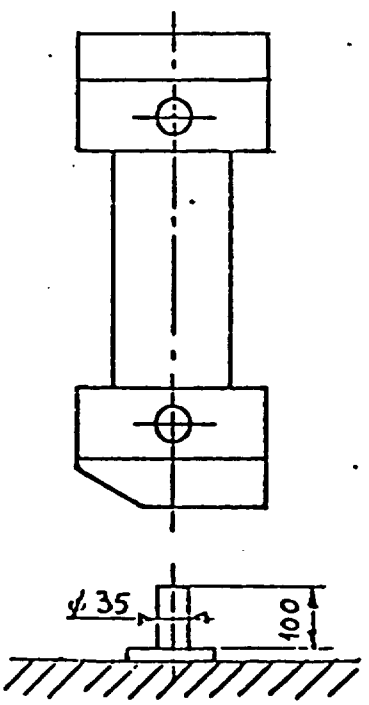	- penetration of punch : 90 mm - casing of cover (4 mm mild steel) punched - bubble test : tight (air pressure at 3,5 bar)	

DROP NR.	DROP	ORIENTATION OF MODEL	RESULTS OF DROP	FIG. Ref.
4	9 m	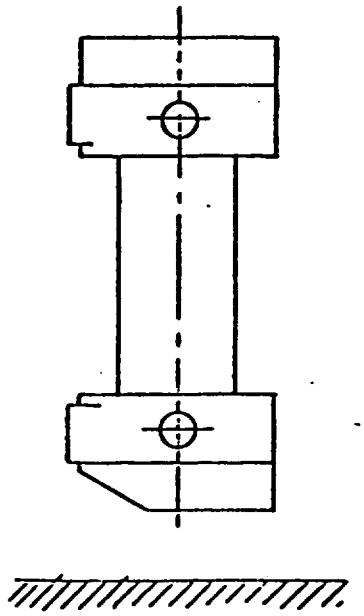	- even squeezing of cover : 10 mm - bubble test : tight (air pressure at 3 bar)	
5	9 m	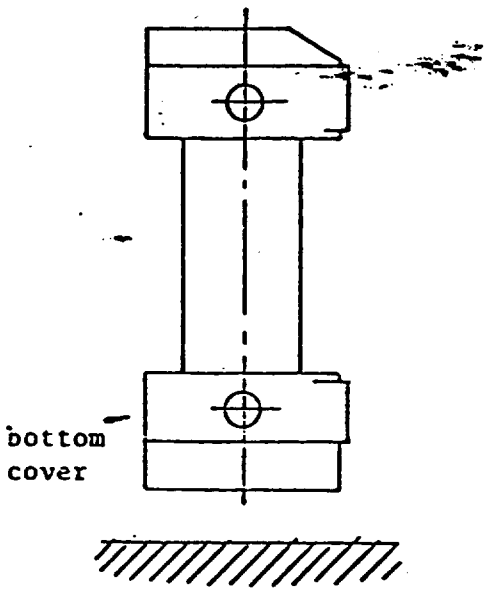	- bottom cover still intact before the test 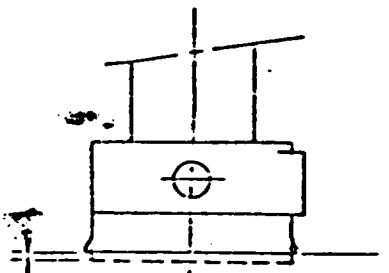 average 15mm max. : 20mm min. : 5mm	5.A.3
6	9 m	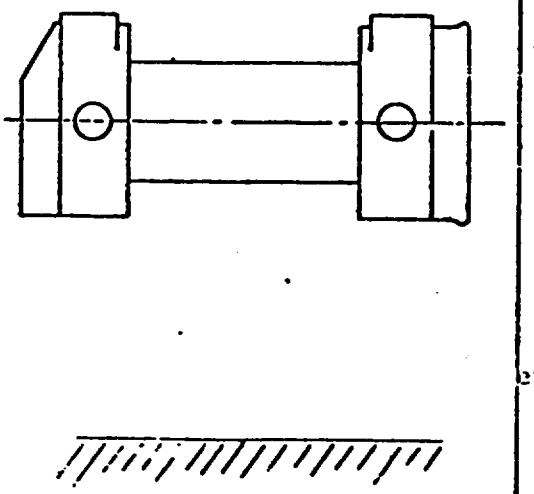	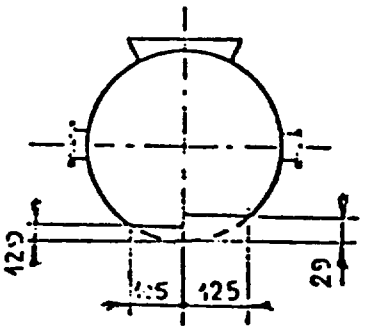 lid extremity bottom extremity	

DROP NR.	DROP	ORIENTATION OF MODEL	RESULTS OF DROP	FIG Ref
7	20 m	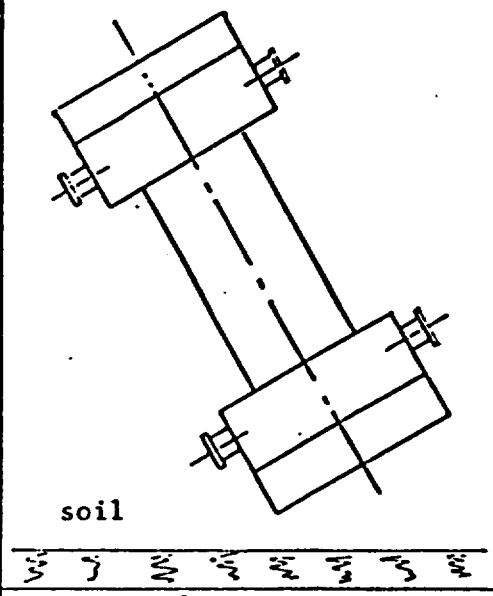 soil	- penetration into the soil: 350 mm max. - no additional damage	
8	20 m	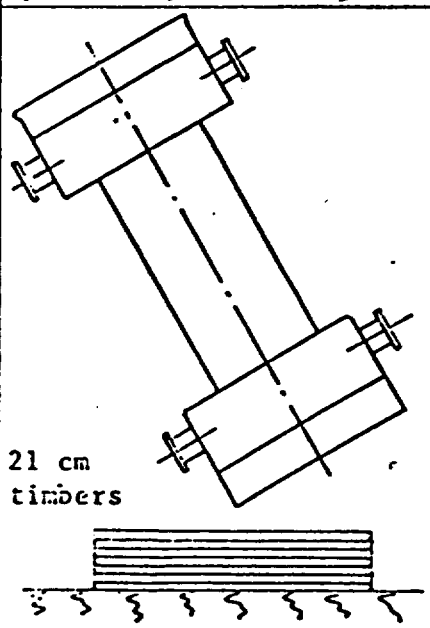 21 cm timbers	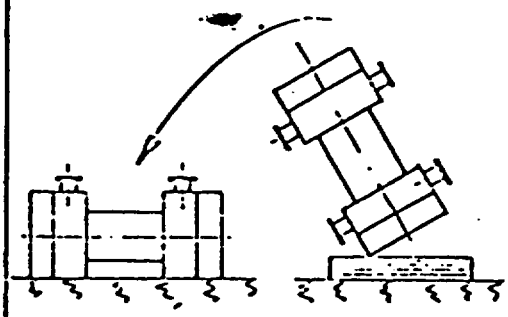 - rebound - no major damage	
9	20 m	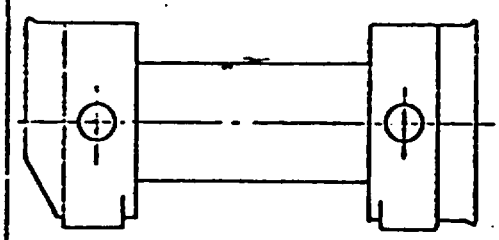 unyielding concrete block 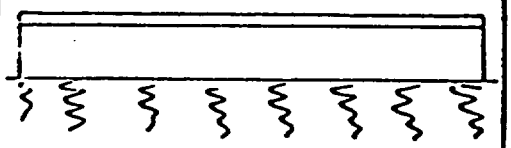	- pronounced squeezing - weld seams in impact area are cracked - practically no bending of the body - only small rebound after the drop	5.A.4

- ANNEX B TO CHAPTER V -

DROP TESTS OF TN9 CASK - HALF SCALE MODEL

Technical

Report

Final Report
F-C3104-1

DROP AND FIRE TESTS OF TN 9 CASK, HALF-SCALE MODEL

PART 1: DROP TESTS, JULY 12-14, 1971

By

G. P. Wachtell

Prepared for

TRANSNUCLEAR, INC.
New York, N. Y.

There is no objection to the use of unclassified test results by you or any other private party in publication, provided that any reference to the source of the test results shall not state or imply any endorsement of the product by the Government, or its agencies, or assumptions by the Government as to the characteristics of articles similar to those tested.

THE FRANKLIN INSTITUTE RESEARCH LABORATORIES
BENJAMIN FRANKLIN PARKWAY • PHILADELPHIA, PENNA. 19103

TABLE OF CONTENTS

		Page
1.	INTRODUCTION	1-1
2.	DESCRIPTION OF MODEL	2-1
3.	TEST PROCEDURE	3-1
4.	TEST RESULTS	4-1
5.	ACKNOWLEDGEMENTS	5-1

1. INTRODUCTION

Drop tests followed by a fire test were performed on a half-scale model of the TN 9 cask, which is a lead-lined shipping container for radioactive spent nuclear fuel, under contract with Transnuclear, Inc., New York, N.Y. The model was supplied by Transnucleaire, S. A. Paris, France.

Through a subcontract with the Naval Air Development Center, (NADC), Warminster, Pennsylvania, facilities of the Naval Air Engineering Center (NAEC), located at the U.S. Naval Base, Philadelphia, Pennsylvania, were used. Close liaison was provided by the NADC staff at the Naval Base.

Under terms of the subcontract the U.S. Government is given the right to reproduce, use and disclose for Governmental purposes this report or any information contained therein. The inclusion of the paragraph on the cover page is also required by the subcontract.

This report describes the drop tests. The fire test is discussed in a separate report.

2. DESCRIPTION OF MODEL

The model was a cylinder 9.4 ft long. Longitudinal copper fins, 6.64 ft long, were attached to the outer steel shell of the lead-lined container. Including the fins, the diameter was 2.54 ft. The steel shell diameter was approximately 1.3 ft. The space between the fins was approximately half-filled with a resin. A dummy payload in the container cavity was provided. This consisted of two concentric steel pipes welded together, weighing a total of 703 pounds.

The finned section and lead filled end pieces were integral parts of the cask. Each end piece had a single flat foot and a pair of lifting trunnions. One foot and one trunnion may be seen in Figure 1, in which the cask is upside down following the first drop test. A shock absorber was bolted to each cask end. The shock absorbers were steel cylindrical containers filled with balsa wood. The model, including the dummy payload, weighed approximatley 9500 pounds. The trunnions were hollow steel cylinders capable of collapsing under severe impact, as verified in the fifth drop test.

3. TEST PROCEDURE

The drop tests were performed on a concrete slab located at the NAEC facility. The slab was 18 inches thick. Part of its area was covered by a high tensile steel plate, 3 in. thick x 5 ft x 20 ft., weighting 122 pounds per square foot.

I-beams were placed across each end of the plate. The ends of the I-beams projected beyond the plate, and were hooked to fixtures embedded in the concrete.

The model was shipped to The Franklin Institute Research Laboratories where it was examined before it was transported to the drop test site. O-rings sealing the inner cover at one end of the cask were found to be in segments. (It was discovered later on that when the model had originally been prepared for shipment, it was thought by those installing the inner cover that the O-rings were needed only for shipping purposes, and not as a gas-tight seal). The O-rings were replaced.

Three "Calrod" electric heating elements, 86 inches long, 4000 watt rating, were connected in parallel and placed inside the inner pipe of the dummy payload. This was done in order to preheat the model before the first drop test. It was originally planned to preheat the model to 230°F, but time did not permit this temperature to be reached. Accordingly, heating was discontinued after the model had been heated for approximately half the time that would have been required, electric leads were cut away, closures in both cask ends were closed, and the shock absorbers were bolted in place.

NAEC photographers took still photographs throughout the series of five drop tests, and also two high-speed motion pictures of each drop test. The drop tests were performed in the following order:

1. Thirty foot drop onto corner, with center of gravity directly over corner and a lead temperature of about 175°F.

2. Thirty foot drop onto same end as in first drop test, axis vertical.
3. Forty inch end drop onto pin. The pin was three inches in diameter. The end was flat, but the edge was rounded. The end was twelve inches from the top of its conical base and seventeen inches from the bottom surface of the base.
4. Forty inch drop onto pin, with cask upside down in a horizontal orientation.
5. Thirty foot drop onto a pair of trunnions with cask in a horizontal orientation.

In the first two tests, the end on which the impact occurred was the one with the inner cover. In the third test, the other end was used.

Two accelerometers were each attached to a model fin for each test except the first and fourth tests, for which only one accelerometer was used. The accelerometers were manufactured by Sensory Products, Cochituate, Massachusetts. They are cylinders, approximately 1/2 inch in diameter and 3-1/2 inches long. The cylinder contains a removable unit in which a small weight rests against a spring. Acceleration causes the weight to compress the spring. The weight is designed to move in only one direction, so that a reading of the peak acceleration is obtained. The reading is permanent until the device is reset. The accelerometers were attached so that they were oriented vertically when the model was falling.

To minimize obscuration by dust when making the high speed motion pictures, the paint was removed from the model in the expected area of impact by means of a solvent, and the top surface of the steel plate was dampened with water. After each test, freon was fed into the cavity and a freon test device was used to search for freon leakage.

4. TEST RESULTS

Previous studies* have shown the validity of impact model testing for lead-lined containers. Figures 1-5 show the external damage due to the tests.

In Figure 1, the partial collapse of the corner of the shock absorber may be seen. The accelerometer reading was 160g.

In Figure 2, the surface of the steel plate shows the circular outline of the shock absorber, as well as the flattened end of the shock absorber itself, after the second test. Figure 5, taken after the fifth test, shows another view of the flattened end. Shock absorber thickness was reduced to 3.5 inches. Both accelerometers indicated 180g.

In Figure 3, the hole made in the shock absorber in the third test is shown. Punch penetration was not more than 6-3/4 inches. The two accelerometer readings were 60g and 20g, respectively. In later examination after the fire test the shock absorber was removed. The inner steel surface was found to have been indented and slightly cracked. This may be partly due to the fact that shims consisting of square washers around each bolt had been provided to allow space for thermocouples that had been installed for the fire test. It had been considered desirable to install these thermocouples before the drop tests so that the shock absorber need not be disturbed between the drop tests and the fire test. Without the shims, the inner face of the shock absorber would have been supported by the cask end. It was also found that the cask end itself was slightly indented. The cask end had two small openings, covered by discs with O-ring seals. One was in the center. The other, fitted with the gas pressurizing connection, was off center. The indentation was

*Clarke, H.G., Jr. (FIRL), *"Impact Resistance of Casks"*, Chem. Engrg. Prog. Symp. Series, vol. 61, no. 56, pp. 30-41, Am Inst. Of Chem. Engrs., New York (1965).

immediately adjacent to the off-center opening, so that the plane of the disc was rotated slightly as a result of the indentation.

Figure 4 shows the hole made in the model in the fourth test. After the fire test, when the shock absorbers and inner cover were removed, visual inspection of the cask cavity showed no apparent distortion of the cavity. The acceleration indicated for this test was 20g.

Figure 5 shows one of the trunnions after the fifth test. Both trunnions had the same general appearance. The indicated accelerations were 180g and 150g, respectively, measured at opposite ends of the cask.

Freon leakage tests made after each drop test showed no evidence of leakage. The presence of a fairly strong breeze created some doubt that a leak would have been detected, although an attempt was made to shield the freon detector from the wind. After the fire test, the model was returned to The Franklin Institute for inspection. Leak tests were conducted indoors. The leak tests were of three kinds:

1. The cavity was found to hold a pressure of 10 psig for 64 hours, with a loss of only 2 psi.
2. "Leak-Tec" was used at all the possible leakage sites. In this method, small bubbles are an indication of a gas leak. No bubbles were seen.
3. The freon test did not disclose any leaks.

The small loss of 2 psi does not indicate a leak, since it is readily accounted for in another way. When the pressure is raised from 15 psia to 25 psia (10 psig), the temperature rises by an amount somewhat less than that corresponding to adiabatic compression. If the initial temperature is 540°R (80°F), adiabatic compression would raise the temperature to $540\ (25/15)^{(\gamma-1/\gamma)}$ (where $\gamma = 1.4$ for air), or 625°R. Subsequent cooling to 540°R would then reduce the pressure to 25 (540/625) or 21.6, a decrease of 3.4 psi.

The initial compression is not completely abiabatic, however, because there is some cooling of the air in the container during the compression. Consequently, the subsequent pressure decrease is less than 3.4 psi.

We conclude that the cask model survived the drop tests satisfactorily.

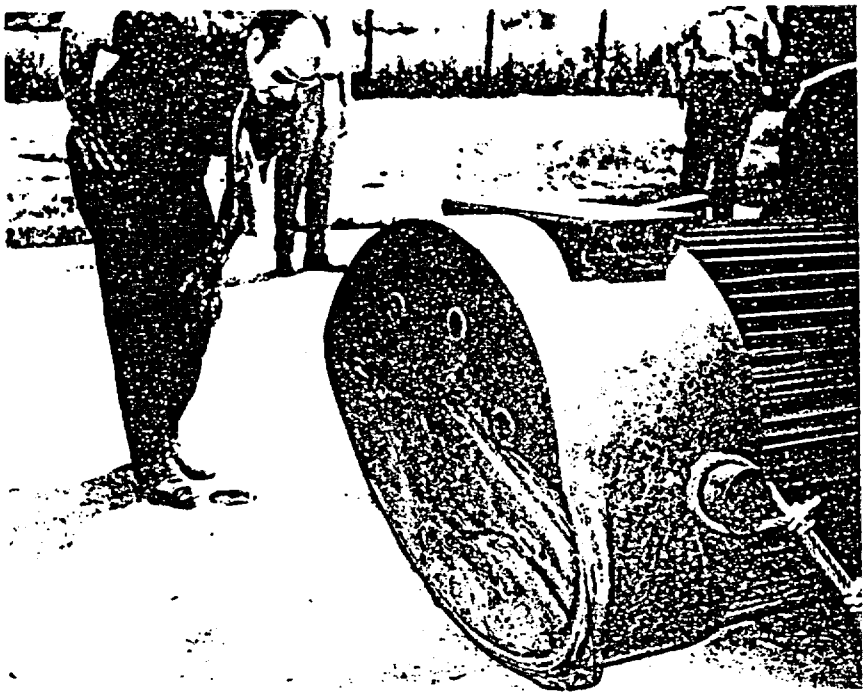

Figure 1.

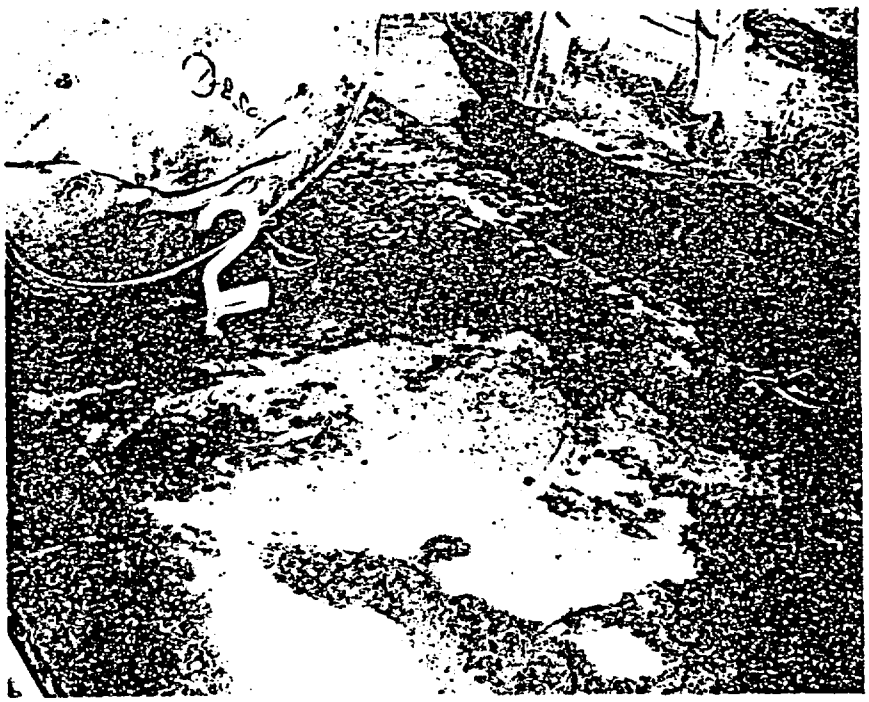

Figure 2.

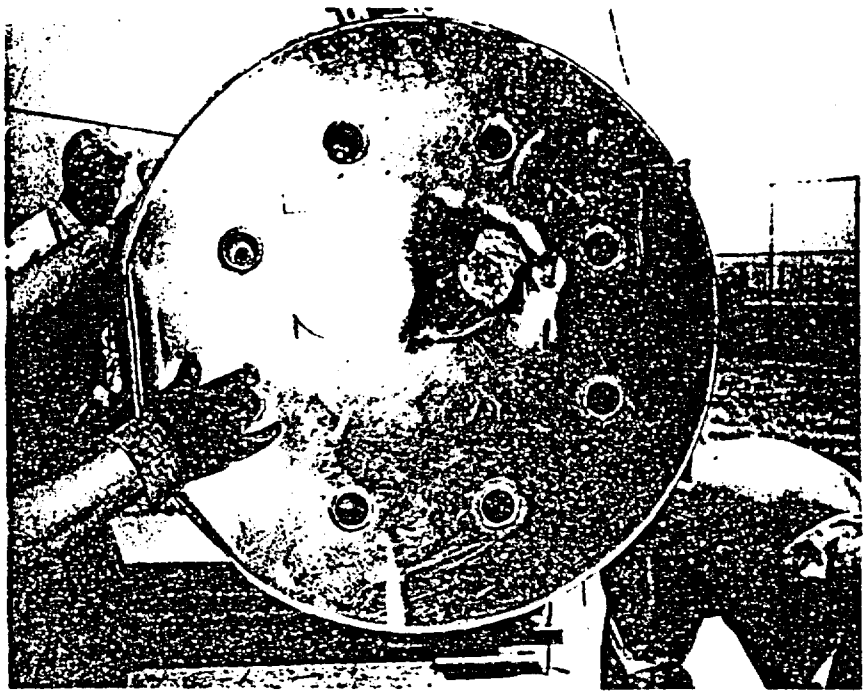

Figure 3.

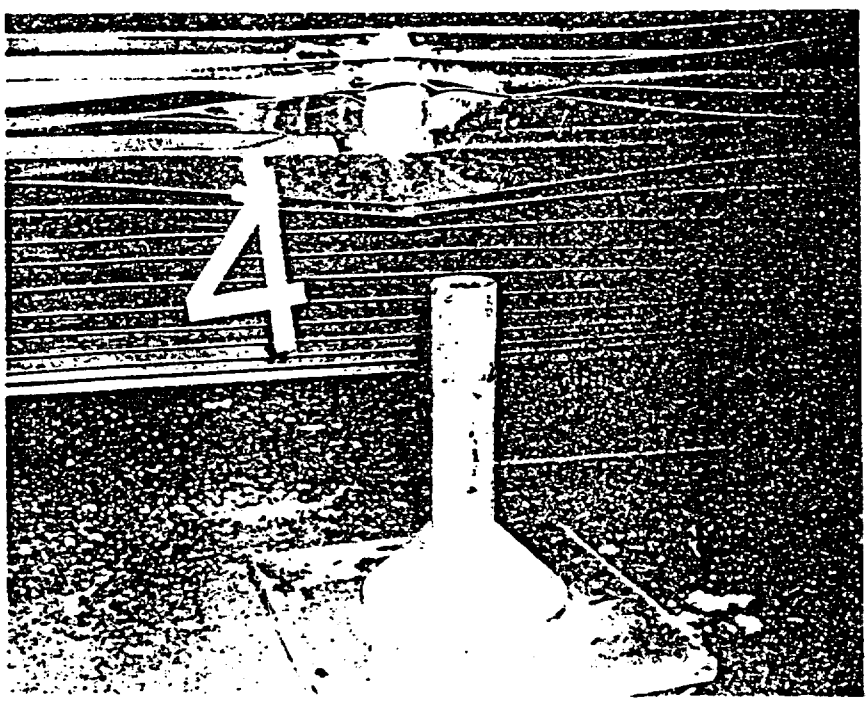

Figure 4.

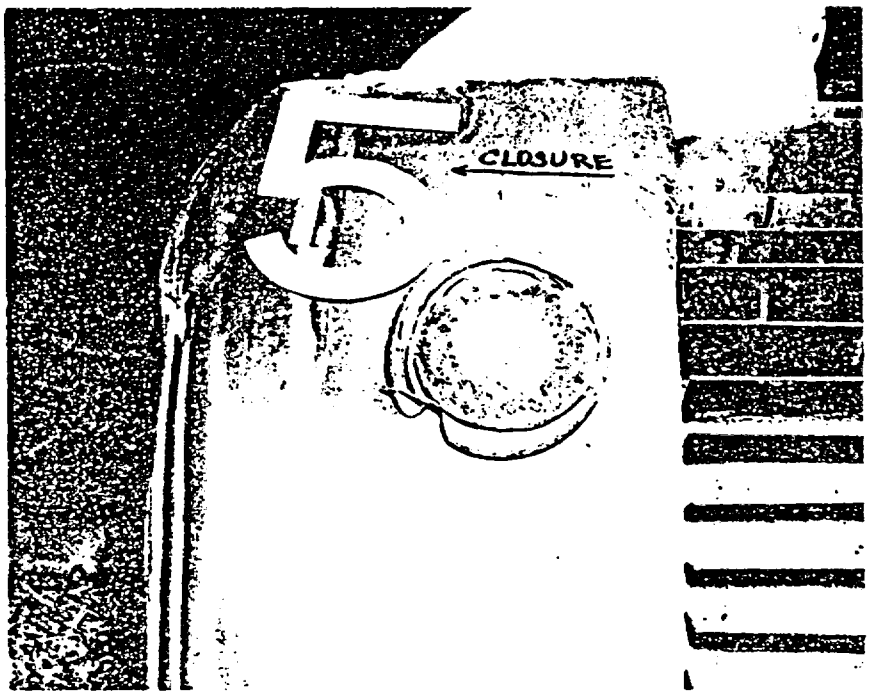

Figure 5.

5. ACKNOWLEDGEMENTS

The NADC staff provided excellent coordination of various groups, including the photographers and the NAEC crew of riggers, whose work was performed expertly and courteously.

The electrically operated release hook was kindly loaned by Eastern Rotorcraft Corp., Doylestown, Pennsylvania. It was their Cargo Release Hook P/N SP7110-1A, Model C100V Serial Number 639, with a 10,000 pound capacity. It worked perfectly everytime.

- ANNEX C TO CHAPTER V -

FIRE TEST OF TN9 CASK, HALF SCALE MODEL

Technical

Report

Final Report
F-C3104-2

DROP AND FIRE TESTS OF TN 9 CASK, HALF-SCALE MODEL

PART 2: FIRE TEST, JULY 15, 1971

By

G. P. WACHTELL

Prepared For

Transnuclear, Inc.
New York, N.Y.

THE FRANKLIN INSTITUTE RESEARCH LABORATORIES
BENJAMIN FRANKLIN PARKWAY • PHILADELPHIA, PENNA. 19103

TABLE OF CONTENTS

		Page
1.	INTRODUCTION	1-1
2.	DESCRIPTION OF MODEL	2-1
3.	THEORY OF SCALE MODELING	3-1
4.	COMPUTED PERFORMANCE	4-1
5.	PREPARATION FOR FIRE TESTS	5-1
6.	PERFORMANCE OF TEST	6-1
7.	RESULTS OF FIRE TEST	7-1
8.	SUMMARY AND CONCLUSIONS	8-1
9.	ACKNOWLEDGEMENT	9-1

LIST OF TABLES

Table No.		Page
1	Quantities Used in Analysis.	4-3

LIST OF FIGURES

Fig. No.		Page
1 to 12.	Photographs	9 to 7
13.	Computational Nodes.	9-8
14 to19.	Calculated Full-Scale Thermal Behavior.Temperature Versus Time	9-14
20.	Calculated Thermal Behavior of Model. Temperature Versus Time	9-15
21.	Test Duration Versus Fire Thermocouple Readings. . . .	9-16
22.	Transnucleaire Full-Scale Model Section.	9-17

1. INTRODUCTION

A series of drop tests and a fire test were performed during July 1971 on a half-scale model of a lead lined shipping container for spent nuclear fuel, under a contract with Transnuclear, Inc., New York. The model was supplied by Transnucleaire, S. A., Paris.

The drop tests were performed first, and were then followed by the fire test. The present report concerns the fire test. The drop tests are described in a separate report.

2. DESCRIPTION OF MODEL

The model* was a half-scale model of the TN 9 cask, with longitudinal fins. Its general features may be seen in Figure 1, photographed immediately following the fire test. The full length of the model was 9.4 ft, including the detachable end pieces, which were shock absorbers. The shock absorbers consisted of short cylindrical sheet metal containers filled with balsa wood. The eight bolt-holes visible in Figure 1 were lined with sheet metal also. (The large hole near the middle resulted from a drop test onto a three-inch diameter pin.) There were two lifting trunnions at each end on the body of the cask. One is visible at the right in Figure 1. The body of the cask also had a supporting foot at each end. These feet rested on pedestals during the fire test, as may be seen in Figure 1 and also in Figure 2, which is a view of the end on which the corner and end drop tests were performed.

The model had 58 longitudinal copper fins 6.64 ft long, 0.57 ft tall and 0.00656 ft thick, attached to a cylindrical sheel of 0.0328 ft thick steel. The outside diameter of the model, including fins, was 2.54 ft. The steel shell housed the lead lining of the model, but was separated from the lead by a layer of insulating cement, 0.0164 ft thick. The composition of the cement was not known by us, but we were informed that it contained water which would be driven off by heat upon the melting of fusible plugs in the vent holes provided for the escape of the water vapor. Normally, the thermal conductivity of the cement is about 1 BTU/ft-hr-°R, but when the water is driven off, the thermal conductivity is reduced by a factor of three.

*The model is shown on Transnucleaire Drawing Number 9085-55 (not included in this report).

The outside diameter of the lead lining was 1.3 ft. The cavity inside the lead was lined with steel, and was roughly octagonal in shape, the sides being tangent to a 0.78 ft circle. (For purposes of thermal analysis, the cavity was approximated as a cylinder of 0.85 ft diameter).

The shock absorbers were bolted to the cylindrical cask ends which were integral with the cask. The cask ends contained the end lead shielding, and were steel shells fitted with the trunnions and feet, and filled with balsa wood.

The end shown in Figure 1, and in Figure 7 after removal of the shock absorber, had two openings, one concentric with the model, and the other off axis. These openings were closed by removable flat covers with O-ring seals. The end shown in Figure 2, and in Figure 12 after removal of the shock absorber, had a removable lead-lined lid containing an opening which was closed by a removable flat cover held by 4 screws, that permitted access to the cavity. Sealing of the lead-lined lid was provided by a pair of Silastic O-rings.

The O-rings were found to have been damaged when the model was delivered. They were therefore replaced by butyl rubber O-rings before the drop and fire tests.

The spaces between the fins were filled with a resin to approximately half the height of the fins.

The model was provided with 2 mm thermocouple wells leading to various locations in the model. Stainless steel sheathed thermocouples were placed between one cask end and its shock absorber, as may be seen in Figures 7 and 9, to permit the thermocouples to be brought out.

Most of the thermocouples were brought out as a group and led away from the cask through a pipe that may be seen in Figure 1. The pipe was sealed to the model by a layer of cement (asbestos with a binder). The lower part of the pipe was also covered by a layer of insulation.

As described later, thermocouple connectors that were housed in the pipe failed early in the fire test, with the result that these thermocouple readings were lost.

Thermocouple wells were also provided at three locations at the interface between resin and steel. These locations were in the vertical midplane of the model, one in the bottom position (lower resin thermocouple) and the other two 120 degrees away (upper resin thermocouples). In addition, a thermocouple well was provided in the cover (i.e. removable inner lid) at the inner (i.e. cavity-facing) surface of its lead filling. To install this thermocouple, a hole was drilled in the shock absorber before the drop tests were performed, permitting the thermocouple to be led out through the protective pipe seen in Figure 2 without the use of shims.

As may be seen in Figure 1, the pipe leading to the upper resin location was provided with a protective layer of cement (asbestos with a binder) where it met the fins. The pipe leading to the lower resin point may be seen to have shifted and lost the cement. Evidently the lower resin thermocouple was damaged by this shifitng, leading to much higher temperature readings than the two upper resin thermocouples. A very rapid rise in the cover thermocouple reading to 1000°F, the maximum of the recorder, which cannot reasonably be accounted for as the temperature in the cover, indicated that this thermocouple suffered damage also.

A thermocouple was also placed directly into the hole made in the end pin drop test, as may be seen in Figure 1. This thermocouple is referred to as the pin hole thermocouple.

A dummy payload was placed inside the cavity for the drop tests and the fire test. It was 88 inches long, and consisted of two concentric steel pipes welded together. The outer diameter of the outer pipe was 8.6 inches, and the inside diameter of the inner pipe was 4.9 inches. The payload weighed 703 pounds.

After the fire test, the various parts of the model were weighed by means of a load cell, leading to a total weight, including the dummy payload, of 9085 pounds. Before the drop tests, the weight indicated by a spring balance supported by a crane was approximately 400 pounds more. The difference is not plausibly accounted for by loss of resin during the fire test, and must be attributed to the use of different weight measuring devices.

3. THEORY OF SCALE MODELING

We compare here the thermal performance of a scale mode (quantities designated by subscript m) exposed to an incoming flux Q_{im} and the full scale object exposed to incoming flux Q_i. With an effective exposed surface temperature T_e, there is an outgoing flux of

$$Q_o = \alpha\sigma\ T_e^4$$

where α is the absorptivity of the surface and σ is the Stefan Boltzmann constant. The net flux $Q_i - Q_o$ adds heat to the object.

We assume that the model is made of materials having thermal conductivity k_m and heat capacity per unit volume $(\rho c)_m$ equal, at any given point in the model, to k and (ρc) at the corresponding point in the full scale object. We also assume that initial conditions are the same.

If at some time t_m after the start of exposure of the model there is to be a temperature distribution similar to that at some time t in the full scale object, then evidently the temperature gradient at any point in the model will be 1/S times the temperature gradient at the corresponding point in the full scale object, where the scaling factor S is d_m/d, d being any typical dimension. Since this must hold true at every point, including points close to the surface, it follows that a prerequisite for exact modeling is

$$(Q_i - Q_o)_m = (1/S)\ (Q_i - Q_o) \tag{2}$$

We also evidently have

$$\left(\frac{\partial^2 T}{\partial x^2}\right)_m = \left(1/S^2\right)\ \left(\frac{\partial^2 T}{\partial x^2}\right) \tag{3}$$

From the equation for heat conduction,

$$\frac{\partial t}{\partial t} = \frac{k}{\rho c} \frac{\partial^2 T}{\partial x^2} \tag{4}$$

along with $(k/\rho c)_m = (k/\rho c)$ it immediately follows that

$$t_m = S^2 t \tag{5}$$

if exact modeling is to be accomplished.

If Q_i and Q_{im} are constants and T_e initially has a low value, so that from equation (1), Q_o is small, equation (2) shows the requirement

$$Q_{im} = Q_i/S \tag{6}$$

This is the basis for undertaking a double-flux experiment with a half-scale model. As T_e increases, Q_o increases to appreciable values, so that equations (2) and (1) require

$$\alpha_m = \alpha/S \tag{7}$$

With an assumed value of $\alpha = 0.8$, we would need to have $\alpha_m = 1.6$ for an exact half-scale model, and this is clearly impossible because α_m cannot exceed unity. To the extent that Q_o is an appreciable fraction of Q_i during some part of the model fire test, the thermal modeling is only approximate.

Assuming that in the real model test, $\alpha_m = \alpha$, some idea of the extent of the modeling error may be obtained by assuming, as a first approximation, that perfect temperature modeling is obtained. The total heat absorbed per unit of external surface area up to time t_m is then actually

$$\int_o^{t_m} (Q_i - Q_o)_m \, dt = Q_{im} t_m - \alpha\sigma \int_o^{t_m} T_e^4 \, dt \tag{8}$$

instead of the amount that would have given exact modeling; namely, the amount computed from the above expression with α/S in place of α. That is, the actual model absorbs too much heat, the factor by which the heat absorbed exceeds that for exact modeling being

$$\frac{Q_{im} - \alpha\sigma\,(T_{em}{}^4)_{av}}{Q_{im} - \frac{\alpha\sigma}{S}\,(T_e{}^4)_{av}} \tag{9}$$

where $T_{em} = T_e$ to a first approximation. Because of this excess net heat absorption, the temperature will be higher in the actual model test than it would be with exact modeling, and this is true on the external surface as well as in the interior. $(T_{em}{}^4)_{av}$ will therefore be higher than $(T_e{}^4)_{av}$, reducing the numerator of (9). In (9), T_e may be regarded as $T_e(t_m)$ for an exact model or as T_e (t) for the full scale object at time $t = t_m/S^2$, since T_e has the same value with either definition.

The amount by which T_{em} exceeds T_e is not so great that numerator and denominator in (9) are equal, for if that were to occur, the net flux in the model would be the correct amount for exact modeling, and in that case T_{em} would equal T_e. We may conclude that the heat absorption in the actual model is excessive by a factor more than unity but less than that given by (9) when T_{em} is taken equal to T_e.

Since the total heat absorbed and the temperature at any point are more in the actual model than in an exact model, a scale model fire test is conservative. That is, if maximum acceptable temperatures are not exceeded in the actual scale model test, with a dimension scaling factor less than unity, we may be confident that they would not be exceeded in a full scale test under standard or reference conditions.

4. COMPUTED PERFORMANCE

According to information communicated by Transnuclear, Inc., the model that was tested was an exact half-scale model in all important details, except for the fins. The fins were longitudinal in the model and approximately circumferential in the full-scale design*. The fin thickness in the model was the same as in the full-scale design, but the number of fins was reduced in the model so that the total mass of copper was the same as that for an exact half-scale model. The actual full-scale fins are cut into strips by radial cuts. The strips are each twisted about a radial axis to separate them, thereby encouraging dissipation of heat by natural convection during normal use. Since heat transfer by radiation is overwhelmingly dominant under fire test conditions, the difference in fin shape is not significant for the present analysis except during cool-down after the fire is extinguished.

To determine full-scale dimensions for computational purposes, dimensions obtained from the drawing of the scale model or (in the case of the length of the cavity) measured directly on the model itself were doubled. This was done for the fins as well as for other parts of the cask, except that the number of fins was doubled and the thickness was kept the same.

The inner surface of the cavity was approximated as a cylinder, the diameter being taken as the mean between a minimum value (237 mm or 9.33 inches for the model) and a maximum value ($\sqrt{237^2 + 156^2}$ mm or 11.17 inches). This mean value is 10.25 inches, taken as the inside diameter of a cylindrical lead tube (the inner cavity steel being taken as lead, for simplicity).

*Figure 22 shows a full-scale model cask section made by Transnucleaire. The fins, originally longitudinal may be seen projecting from the resin after being cut and twisted into the circumferential orientation.

The quantities used in the analysis are presented in Table 1.

We now consider the cask to be a long cylinder and consider a portion between two planes, normal to the axis, separated by one foot.

For purposes of this analysis, the cask is taken to consist of a thickwalled lead cylinder of inner and outer diameters D_{iL} and D_{oL}, covered by a layer of insulating cement of thickness δ_i. The cement fills the space between the lead and the steel outer jacket of the cask, the thickness of the steel being δ_s. Longitudinal copper fins of thickness δ_f and height h_f extend radially from the steel. A resin fills the space between the fins to a depth of h_u measured from the surface of the steel. The exposed height of the fins is $h_e = h_f - h_u$. The resin thermal conductivity is neglected compared to that of the copper fins.

The insulating cement contains water that is allowed to escape through vent holes when fusible plugs melt. This occurs at 186°C (367°F). The escape of the water is by evaporation. Latent heat of vaporization was neglected in the calculations. This neglect is conservative. The evaporation of the water decreases the thermal conductivity by a factor of about 3. (The values of k_i given in Table 1 are converted from the values 1.5 (wet) and 0.5 (dry) kcal/h m °C. The number of decimal places retained in Table 1 was only for computational purposes, and does not represent the precision with which k_i is known).

To set up a computational model, the procedure adopted was to establish nodes representing heat capacities, separated by heat flow resistances. Figure 13 shows the arrangement of nodes.

For one foot of cask length, the rate at which heat enters the exposed fins by radiation is $\pi D_f (Q_i - Q_o)$. The fin cross sectional area for conducting heat radially inward is $N\delta_f$. The node representing the exposed fins was taken to be midway between the outer resin surface and the outer edge of the fin.

Table 1

QUANTITIES USED IN ANALYSIS

Quantity	Symbol	Value: Full Scale	Value: Model	Dimensions
Fire Emissivity	ε	0.9	0.9	
Surface Absorptivity	α	0.8	0.8	
Stefan-Boltzmann Constant	σ	0.173×10^{-8}	0.173×10^{-8}	$BTU/ft^2hr°R^4$
Incoming Flux	Q_i	17462	34924	BTU/ft^2hr
Fin height	h_f	1.148	0.574	ft
Unexposed fin height	h_u	0.590	0.295	ft
Exposed fin height	h_e	0.558	0.279	ft
Number of fins	N	116	58	
Density of fin material (copper)	ρ_f	555	555	lb/ft^3
Specific heat of fin material	c_f	0.094	0.094	BTU/lb°R
Thermal conductivity of fin material	k_f	242	242	BTU/ft hr°R
Fin thickness	δ_f	0.00656	0.00656	ft
Thickness of insulating cement	δ_i	0.0328	0.0164	ft
Thermal conductivity of cement	k_i	0.336(dry) 1.008(wet)	0.336(dry) 1.008(wet)	BTU/ft hr°R
Density of Steel	ρ_s	487	487	lb/ft^3
Specific heat of steel	c_s	0.125	0.125	BTU/lb°R
Thickness of steel	δ_s	0.0656	0.0328	ft
Density of lead	ρ_L	687	687	lb/ft^3
Specific heat of lead	c_L	0.0325	0.0325	BTU/lb°R
Thermal conductivity of lead	k_L	18.6	18.6	BTU/ft hr°R
Outside diameter (envelope around fins of cask)	D_f	5.08	2.54	ft
Outside diameter of lead	D_{oL}	2.6	1.3	ft
Mean inside diameter of lead	D_{iL}	1.7	0.85	ft
Lead thickness, $(D_{oL}-D_{iL})/2$	δ_L	0.45	0.225	ft
Melting point of lead	T_m	$\begin{Bmatrix}621\\1081\end{Bmatrix}$	$\begin{Bmatrix}621\\1081\end{Bmatrix}$	$\begin{Bmatrix}°F\\°R\end{Bmatrix}$

The unexposed part was divided into four segments of equal length, the node for each segment being placed at the middle of the segment. The heat capacity assigned to a node was the total heat capacity per foot of cask length for the segment represented by the node. The heat flow resistance between successive nodes was the sum of two terms, each term being the heat flow resistance from the position of the node to the segment's end closest to the other node. Thus, for example, the exposed fin loses heat to the unexposed portion, per foot of cask length, at the rate

$$N(k\delta)_f\ (T_1 - T_2)/(h_e/2 + h_u/8).$$

The steel was divided into three segments of equal mass, and the lead was divided into four segments of equal mass. For a steel segment or a lead segment, the position (radial coordinate) of the node, and the heat flow resistance from the node to the inner or outer radius of the segment, were determined in accordance with the following derivation. Let r_a and r_b be inner and outer radii of the cylindrical surfaces of the segment. We seek a suitable definition of r_n, the radial coordinate of the node. Suppose that we start with a steady temperature distribution and then change the temperatures T_a and T_b at r_a and r_b to new constant values. The resulting transient will be followed by a new steady temperature distribution. The quantity of heat that is added to the segment is $\overline{C}\Delta T_{av}$ where $\overline{C}$ is the total heat capacity of the segment. The computed value of the added heat is $\overline{C}\Delta T_n$. (The symbol $\overline{C}$ is used here because the symbol C is used later with another meaning). This computed value will be correct if r_n is defined so that under steady conditions, $T_n = T_{av}$.

With cylindrical geometry, this leads to the formula

$$\ln r_n = \frac{r_b^2 \ln r_b - r_a^2 \ln r_a}{r_b^2 - r_a^2} - \frac{1}{2}$$

The heat capacity of the segment per unit length of cask is readily shown to be

$$\overline{C} = (\rho c)\ \pi\ (r_b^2 - r_a^2)$$

where c is the specific heat, so that ρc is the heat capacity per unit volume. The heat flow resistance between two cylindrical surfaces between which k is constant, for example at $r = r_n$ and $r = r_m$, is

$$R_{nm} = \frac{\ln r_n/r_m}{2\pi k}$$

where r_n must be taken > r_m so that R_{nm} is positive.

For node numbers i (except for the first and last nodes) the temperature increase during a short time interval Δt is

$$\Delta T_i = (A_i\ T_{i-1} + B_i\ T_i + C_i\ T_{i+1})\Delta T \quad (1 < i < 13)$$

where

$$A_i = R_{i-1,i}/\ \overline{C}_i,\ C_i = R_{i,\ i+1}/\ \overline{C}_i, \text{ and } B_i = -\ (A_i + C_i)$$

As in the case of the unexposed fin nodes, $R_{i,i+1}$ is the sum of two terms, except that for R_{89} there is an additional term $\delta_i/(k_i\ \pi\ D_{oL})$ representing the heat flow resistance of the insulating cement.

When the temperature of the inner steel node (node number 8) reaches the melting point of the fusible plugs (T_{crit} = 367°F) the values of B_8, C_8, A_9, and C_9 are changed from the values computed with the "wet" thermal conductivity of the cement to the values computed with the "dry" thermal conductivity.

Node number 13 represents the payload, assumed to be concentrated on the inner surface of the lead. Thus, $R_{12,\ 13}$ consists of only one term, corresponding to the lead between the inner surface of the lead and node number 12. For the payload,

$$\Delta T_{13} = (A_{13}\ T_{12} + B_{13}\ T_{13} + D_2)\Delta t$$

where D_2 represents the internal heat generation of the payload. For the model, $D_2 = 0$. For the full-scale cask,

$$D_2 = Q_{self} / \overline{C}_{13}$$

Here $\overline{C}_{13}$ was taken to be 47.93 BTU/°F per foot of full-scale cask (based on the model payload, which weighted 703 pounds and was 88 inches long, with specific heat taken to be 0.125 BTU/lb°F). Computations were carried out for two values of Q_{self}, the payload self-heating rate in BTU/hr per foot of cask.

The larger, or "peak" value of Q_{self} was the value required to sustain a temperature difference of 39.6°F between inner and outer lead surfaces. This temperature difference corresponds to the range of initial temperatures in the lead (113°C to 135°C) given in information supplied by Transnuclear, Inc.

The peak value of Q_{self} is 10892 BTU/hr per foot, leading to $D_2 = 227.25$.

The smaller, or "average" value of Q_{self} was the value 6.65 kw/m, or 6919 BTU/hr per foot, supplied by Transnuclear, Inc. This leads to $D_2 = 144.36$.

It may be argued the "peak" value of Q_{self} is significant only in establishing the initial steady temperature distribution, and that the "average" value should be used in calculating the transient temperature during and after the fire, since the average value represents all the heat generated by the payload. On the other hand, if axial heat conduction is not substantial, the maximum lead temperature will correspond to the peak

value of Q_{self}, occurring in the midplane of the payload where heating is more concentrated.

Strictly speaking, the problem is three-dimensional, since axial conduction may not be negligible. The use of the higher value of Q_{self} is clearly conservative. Results of calculations with both values are presented.

For the first node, representing the exposed fins

$$\Delta T_1 = (B_1 T_1 + C_1 T_2 + D_1 + E (T_1 + 460)^4 - D_3 (T_1 - T_{amb}))\Delta t$$

where $C_1 = - B_1 = R_{1,2} / \overline{C}_1$. D_1 represents the effect of radiant heat addition from the fire.

$$D_1 = \pi D_f Q_i / \overline{C}_1 \quad (t < t_f)$$

$$D_1 = 0 \quad (t \geq t_f)$$

where t_f is the duration of the fire. The incoming flux Q_i is given in Table 1. Note that Q_i is twice as large for the model as for the full-scale cask. In accordance with the theory of scale modeling discussed earlier, this should yield exact thermal modeling, except for the effect of the following:

1. Q_o is not negligible compared to Q_i.
2. During cool-down, h should be twice as large for an exact scale model as for the full-scale cask. For the model with half the number of fins, h should be larger by still another factor of 2. In the calculations, however, the same value of h was used in both cases.
3. There was no self-heating of the model payload.
4. Initial temperatures were slightly different. The initial temperature in the model approximated that for the actual fire test. In the full-scale calculation, the initial temperature distribution was that corresponding to the peak value of Q_{self}.

The initial conditions were taken to be the following:

For the model, all nodes were initially at 90°F. T_{amb} was also 90°F.

For the full-scale cask, the initial temperatures were calculated from the initial lead temperatures and the temperature drops due to the peak value of Q_{self}. T_{amb} was taken to be 100.4°F (38°C). The heat flow resistance of the wet insulating cement at its nominal thickness (10mm full-scale) was used in determining initial conditions. The same initial conditions were then used for thermal transient calculations with larger and smaller cement thicknesses. The initial temperatures for the full-scale cask were as follows:

Node Number	Location	Initial Temp (°F)
1	Exposed fin	140
2	Unexposed fin	150
3	Unexposed fin	160
4	Unexposed fin	170
5	Unexposed fin	180
6	Steel	190
7	Steel	190
8	Steel	190
9	Lead	240
10	Lead	250
11	Lead	260
12	Lead	270
13	Payload	275

Dissipation of the peak value of Q_{self} and an assumed solar heat load of 4 kw for the full length of the finned portion of the cask would require a heat transfer coefficient (natural convection plus radiation) of about 2.4 BTU/hr ft^2 °F to yield the exposed fin temperature of 140°F. In calculating the cooldown behavior, the heat transfer coefficient was taken to be h = 1.0 BTU/hr^2°F, a reasonable value for the effect of natural convection alone.

A digital computer program was prepared to perform the calculations. Any number of nodes can be used, up to a maximum of 50, and this maximum can be increased by a minor change in the program. The value of the time step Δt can be given any value, and the computation can be continued for any desired number of time steps. Thus, the program can be used for thermal transient calculations on other casks of approximately similar design, This flexibility made it possible to investigate the behavior of the full-scale cask with assumed (6 mm) and maximum (14 mm) cement thicknesses, to allow for possible tolerances in this dimension.

Although the program permits an arbitrary choice of Δt, accuracy requires that Δt be chosen small enough. If the number of nodes is increased, Δt must be taken smaller, by a factor equal to the square of the factor by which the number of nodes is increased. The reason for this is that $R_{i-1,\ i}\ \overline{C}_i$ is a time-constant for charging the heat capacity $\overline{C}_i$ with heat from node number i-1, and Δt should be small compared to this and similar time constants. Otherwise the average heat flow rate through $R_{i-1,\ i}$ during the time interval Δt will differ substantially from the heat flow rate at the start of the time interval. Since $R_{i-1,\ i}$ and $\overline{C}_i$ are both inversely proportional to the number of nodes, the maximum value that should be used for Δt is inversely proportional to the square of this number.

In carrying out the computations, Δt was taken to be 0.00025 hrs for the full-scale cask and 1/4 as large for the model.

The results of the calculations are shown in Figures 14-20, inclusive.

In Figures 14 and 15, the nominal (10 mm) thickness of cement was used. In Figure 14, the peak value of Q_{self} was used, and in Figure 15, the average value was used. The fire duration was 0.5 hrs. The maximum lead temperature is that of the payload, 530°F at t = 1.3 hrs in Figure 14 and 498°F at t = 1.2 hrs in Figure 15. The difference is due to the difference in values taken for Q_{self}. In both cases, the temperature remained well below 621°F, the melting point of lead.

In Figures 16 and 17, the minimum cement thickness (6mm) was assumed, with Q_{self} taken at peak and average values, respectively. Compared to the behavior with 10 mm cement thickness, the lead is heated more rapidly during the fire but also cools more rapidly afterwards. In Figure 16, the maximum lead temperature occurs at the payload, 561°F at 1.1 hrs. In Figure 17, with the smaller self-heating value, the maximum payload temperature, 530°F at t = 1.0 hrs, is slightly exceeded by the maximum temperature of the outer lead node, 534° at 0.65 hrs. Using the temperatures at the two outer lead nodes to perform an extrapolation, the outer surface of the lead is about 10°F warmer than this value. Evidently the increased lead heating rate during the fire outweighed the moderate increase in the maximum lead temperature.

In Figures 18 and 19, the cement thickness was taken to be 14 mm, with Q_{self} equal to its peak and average values, respectively. The maximum lead temperature again occurs at the payload, representing the inner surface of the lead. This is 521°F at t=16 hrs. in Figure 18 and 478°F at t = 1.4 hrs in Figure 19. Evidently the decreased lead heating during the fire outweighed the decreased cooling rate during cooldown. The maximum temperature is seen to be more sensitive to the value of Q_{self} when the cement thickness is larger.

Figure 20 shows the results of the model. The fire duration was taken to be 0.1725 hrs (10.35 minutes) to represent the fire duration during the actual fire test. Q_i, the incoming flux, was twice as large as with the full-scale cask. Note that the time scale is altered by a factor of 4, compared to Figures 14-19. The maximum lead temperature is calculated to be 509°F at 0.325 hrs. The fire duration was 1.38 times as long as the duration (0.125 hrs) that theoretically should be used to model a 0.5 hr exposure of a full-scale cask. This extra duration, according to the calculations, approximately compensated for the lack of payload self-heating, as far as maximum lead temperature is concerned.

The calculated maximum lead temperatures are summarized below:

Cement Thickness (mm)	Q_{self} (BTU/hr) per ft of cask	Maximum Lead Temperature (°F)	Time (hrs.)
10	Peak	530	1.3
10	Average	498	1.2
6	Peak	561	1.1
6	Average	544*	0.6
14	Peak	521	1.6
14	Average	478	1.4
5 (Model)	None	509*	0.325

*Lead outer surface

In all cases, the calculated maximum lead temperature is seen to be well below 621°F, so that there is no risk of lead melting.

5. PREPARATION FOR FIRE TESTS

The fire test was performed at the Naval Damage Control Training Center, United States Naval Base, Philadelphia, Pa. Permission to use the facilities, and the assistance of the staff of the Training Center, are gratefully acknowledged.

The fire basin consisted of a square sheet metal container with water-cooled walls. The interior was an 18-foot square. The walls were 30 inches high. After the model was placed on the test stand and thermocouples were installed, the basin was filled with water to a depth of about two feet. Number two fuel oil was added to an additional depth of four inches, so that the fuel surface was about two inches below the top of the wall. Five gallons of gasoline were added shortly before ignition, to ensure rapid spread of the flame.

As may be seen in Figure 1, the test stand consisted of a pair of pedestals on which the feet of the model rested, and was located so that the center of the model was over the center of the basin. The pedestal surface was 58 inches above the basin floor, or 30 inches above the initial fuel surface.

A frame composed of two-inch pipe provided support for thermocouples for measuring the fire temperature. Ten thermocouples were provided as follows:

Eight were in the vertical midplane containing the axis of the model, at the corners and the midpoints of the sides of a rectangle. The sides of the rectangle were one foot from the model. (At the end seen in Figure 2, the one-foot distance is with respect to the shape that the shock absorber would have had if it had not been crushed in the drop tests).

Two thermocouples were placed at the elevation of the axis, in the midplane perpendicular to the axis, one at each side of the model. These were also one foot from the model.

The fire temperature thermocouples were stainless steel sheathed, 1/16 - inch in diameter. (The thermocouples inserted into the thermocouple wells in the model were 1/32 - inch in diameter). All projected from 1/4-in. steel protection tubes, except the lowest one at one end, as may be seen in Figure 2. This thermocouple was covered with a steel cylinder, one inch long and one inch in diameter, intended to average out any rapid fluctuations in fire temperature. Similar cylinders were originally provided for the other fire thermocouples, but were removed because it was thought to be possible that they would produce too large a time lag for a test of very short duration (nominally 7.5 minutes).

Two temperature recorders were used: One, manufactured by Honeywell, printed 12 thermocouple readings in sequence, at the rate of 30 readings per minute, and had a range of 0 to 2400°F. The other, manufactured by Leeds & Northrup, also printed 12 readings in sequence, but at the rate of 12.5 readings per minute, and with a range of 0 to 1000°F. The thermocouples were chomel-alumel. All the fire thermocouples were connected to the Honeywell recorder. In addition, the lower resin thermocouple and the upper resin thermocouple hidden from view in Figure 1 were connected to this recorder. All the other thermocouples were connected to the Leeds and Northrup recorder.

Temperature indications were also obtained from "Tempilstik" markings placed on various locations in the model just prior to the drop tests. These are crayon markings that lose their color when heated above their transition temperatures. Five crayon markings were placed in a group, having transition temperatures of 400, 450, 500, 550 and 600°F.

6. PERFORMANCE OF TEST

As explained earlier in this report, the fire test was nominally a double-flux test. That is, ideally, the test should have twice the incoming flux that would occur with a fire temperature of 1475°F and an emissivity of 0.9.

To anticipate the possibility that the flux would be less than double, it was planned to terminate the test after a duration that would be quickly determined from the fire temperature readings. It was considered undesirable to prolong the test beyond the duration that would compensate for the fire temperature, because that would lead to the risk of causing a failure of the model even though it might have passed an accurate test.

Expressing temperatures in °F, we have for the equilibrium temperature T_{tc} of a thermocouple in a fire of temperature T_f:

$$0.9\ (T_f + 460)^4 = (T_{tc} + 460)^4$$

We assume that the desired fire duration is such that the total heat delivered is the same as in the ideal double-flux case. That is, t should be inversely proportional to $(T_{tc} + 460)^4$ and should be 7.5 minutes in the double-flux case.

In the double-flux case,

$$(T_f + 460)^4 = 2\ (1475 + 460)^4,$$

leading to $T_{tc} = 1781$ °F. Thus,

$$t = 7.5\ \frac{1781 + 460}{T_{tc} + 460}\ \text{minutes}$$

This equation is plotted in Figure 21.

This led to the following table for making a rapid decision for test termination:

Average Thermocouple Indication (°F)	Test Duration (min.)
>1780	7.5
1745 - 1780	8.0
1710 - 1745	8.5
1680 - 1710	9.0
1650 - 1680	9.5
1625 - 1650	10.0
1600 - 1625	10.5
1575 - 1600	11.0
1555 - 1575	11.5
1535 - 1555	12.00

During the test, there was little time to average the thermocouple readings. The decision to call for termination of the test was based on the impression at the time that the readings appeared to have some average value. The foregoing table was essential in making this decision.

The precise duration of the fire test is, of course, a matter of definition because it took a few seconds for the fire to spread when it was ignitied, and a few seconds to extinguish it. The fire was extinguished (Figure 4) with truly amazing speed by the expert application of a fine water spray, taking care not to direct the spray against the model. Taking the timing uncertainties into account (for example, disregarding most of the initial build-up of the fire) the total test duration was 10 1/3 minutes.

Two minutes after the fuel oil fire was extinguished, the resin was observed to be burning, and the model itself was then doused with water.

As mentioned in the description of the test preparations, most of the thermocouples installed in the model failed early in the test. Thermocouple connectors in the pipe in the foreground of Figure 1 were destroyed (Figure 6) by overheating and charring. This resulted in short-circuiting the thermocouples. (It had been planned to bring the pipe away from the model longitudinally, which would have placed the connectors outside of the fire. Unfortunately, this precaution was overlooked at the time of installation, and the pipe was brought out to the side.) In addition, the lower resin thermocouple was damaged by shifting of its protective pipe, the pin-hole thermocouple sagged and fell out of the pin hole, and the thermocouple in the cover (Figure 2) read unreasonably high (1000°F, the maximum of the recorder, after 4 minutes), probably because the thermocouple lead wire was scorched by flames that curled down to ground level in the wake of the basin wall due to the wind.

Thus, the only reliable thermocouple readings in the model were from one of the two upper resin thermocouples.

The fire thermocouples all appear to have survived, except for the upper thermocouple near the end of the model seen in Figure 2.

7. RESULTS OF FIRE TEST

After the fire test, the model was returned to The Franklin Institute Research Laboratories for examination. A side view is shown in Figure 5. The model was pressurized to 10 psig and allowed to stand for 64 hours, during which time the pressure fell to 8 psig, a negligible rate of loss*. In addition, "Leak-Tek" was used in a search for leaks. No bubbles were found; this indicated the absence of substantial leakage. Finally, freon was added to the air in the cavity. A sensitive freon test device, capable of detecting small traces of freon, was used to search for leaks. Again, no leaks were found. The conclusion is that the combination of drop and fire tests did not violate the leak-tightness of the cavity.

Both shock absorbers were removed. The one on which the corner and end drops had been performed was difficult to remove because the metal tubes housing the bolts had collapsed. This shock absorber was dissected and the balsa wood was examined. Substantial charring occurred, as may be seen in Figure 11. More important, however, is the fact that much - perhaps half - of the balsa wood was not charred. This shows that the shock absorber protected the cask end from direct end-wise attack by the fire well enough to prevent the lead in the inside cover from being heated to its melting point.

The inside cover was removed with great difficulty. This may be attributed to the combination of three causes: First, the drop and fire tests caused a slight distortion of the cask end. Second, there was a fairly close clearance in the fit of the cover into the cask end. Third, the cover and hole were cylindrical. The difficulty could be avoided by providing jack screws, and by use of a slight taper in the cover and the hole.

Visual examination of the cavity disclosed no indication of distortion. This supports the conclusion that no substantial melting of lead occurred.

*The loss in pressure is discussed more fully in Part 1 of this report, in which the drop tests are reported.

The fire thermocouple readings were interpreted by calculating a mean radiation value for each thermocouple. That is, for a given thermocouple with T_i representing reading number i in °F, its mean temperature was found as

$$T = \frac{1}{n} \sum_{i=1}^{n} (T_i + 460)^4 - 460$$

where n is the number of readings for that thermocouple during the fire test. This constant value of T would yield the same total heat input as the actual time-varying temperature.

As viewed in Figure 2, the thermocouples and their radiation mean temperatures (°F) were as follows:

Corner thermocouples:

Lower left	926
Upper left	1284
Upper right	Failed
Lower right	949

Opposite the ends of the cask:

Left	1981
Right	1505

Around middle of cask:

Above cask	1737
Below cask	1525
Level with centerline, Visible	1525
Level with centerline, hidden from view by cask	1497

During the tests there was a light breeze of varying intensity generally in the direction toward the camera in Figure 2, or away from the camera in Figure 3. Occasionally, the wind was strong enough so that in the Figure 3 view, the end of the cask was sometimes clearly visible.

The corner thermocouple readings are much lower than the others, indicating substantial dependence of temperature on position.

The radiation mean of the four thermocouple readings around the middle of the cask is 1579°F. From Figure 15, this corresponds to a test duration of 10.9 minutes, or about 0.5 minutes longer than the actual test duration. However, the temperature above the cask was high enough so that the region of the two upper resin thermocouples was exposed just a little longer than necessary. These resin thermocouple readings are therefore valid indications of performance.

Furthermore, the thermocouple opposite the left end, on which the pin drop was performed, had a higher reading than needed for the actual test duration.

For the upper resin thermocouple hidden from view in Figure 2, the temperature reading rose gradually to 800°F at t = 8.3 min., approx., and then fell slowly to 700°F by the end of the test. For the upper resin thermocouple on the side toward the camera in Figure 2, the temperature reading rose gradually to 486°F shortly before the test ended, and then fell to 480°F by the end of the test. These readings may be compared with the calculated steel temperatures, T_s, for the model, shown in Figure 20. The higher peak reading (800°F) is about 375°F lower than the calculated temperature of the steel at the instant when the incoming flux is reduced to zero. The lower peak resin thermocouple reading is about 700°F lower than the calculated value.

The measured steel temperatures indicate that the maximum temperature that occurred in the lead was far below the melting temperature of lead. The fact that the measured temperatures were lower than the calculated steel temperatures may be due to resin decomposition. The resin evolves gases that may help to keep the fins somewhat cooled. For example, if smoke from the resin is cooler than the fire, it will intercept some of the radiation from the fire. Furthermore, endothermic decomposition of the resin would help to protect the steel.

In addition, these were substantial variations in fire temperature, which was generally lower than that needed for a doubled flux.

In Figure 7, the cask end on which the pin drop was performed is shown after the shock absorber was removed. Figure 8 is a close-up view of the same area. The two small closure discs may be seen, the lower one being fitted with the gas connection. The area immediately above the lower disc was indented slightly by the pin drop test. The inner face of the shock absorber is shown in Figure 9, which has been turned 90 degrees so that the bottom of the shock absorber is at the bottom of the photograph. The area of the indentation is clearly visible in Figure 9, and in Figure 10 in which the same area is shown in a close-up view. These figures also show a crack in the indented area, through which hot gases could penetrate to the space between the cask end and the shock absorber.

The occurrance of the crack was undoubtedly encouraged by the use of the shims. Normally, shims would be absent and the shock absorber steel inner face would be better supported by the cask end.

"Tempilstik" markings were visible on the cask end and on the shock absorbers. In the area just to the left of the upper small closure in Figure 8 (located on the model axis) the markings for 450°F and above survived, indicating that the maximum temperature was between 400 and 450°F. In the upper left area in Figure 9, near the edge of the shock absorber, the markings indicated a maximum temperature between 450 and 500°F.

In Figures 7, 8, 9, and 10, strips of masking tape may be seen. This tape was used to hold the shims in place before the shock absorber was attached. Most of the tape survived without being scorched.

The inner cover is shown in Figure 12 before it was removed from the cask. When it was removed, the butyl rubber O-rings were visually inspected and judged to be in excellent condition.

Taken together, all of these observations (balsa wood, masking tape, O-rings, and "Tempilstik" markings) lead to the conclusion that the shock absorbers shielded the cask ends from the fire so that cask end temperature remained well below the melting point of lead at all times.

8. SUMMARY AND CONCLUSIONS

A double-flux fire test of a half-scale model is conservative, because reradiation is not doubled, so the net absorbed flux is more than doubled. The test that was performed differed from a true double-flux test in the following ways:

1. Initial temperature and internal heating of the payload were not simulated.
2. The test duration was longer than the 7.5 minutes that would be needed in a double-flux test, to compensate for the fact that the actual test fire provided less than a double-flux.

Two thermocouples on the model performed satisfactorily. These were located on the interface between resin and steel, and read several hundred degrees lower than the temperature calculated for the steel in a double-flux experiment. A discrepency of this order of magnitude can be explained as due to endothemic decomposition and evolution of gases by the resin, and also by the fact that the fire temperature varied from one point to another and was generally lower than that for a doubled flux.

All indications showed that the lead temperature remained well below the melting point throughout the model. The cavity remained leak-tight. Although some melting of lead should not be expected to damage the cask, the test did not determine whether melting would have done any harm.

Calculations of the thermal performance of the model in a double-flux experiment and of the corresponding full-scale cask in the correct experiment, show that the maximum temperature of the lead is at least 60°F below the melting point in both cases, even with the most unfavorable choices of cement thickness and self-heating in the full-scale cask calculation.

Early dousing of the model was necessary because the resin continued to burn after the fire was extinguished. The resin composition should be modified so that it does not continue to burn; alternatively, experimental or calulational assurance should be provided to ensure that continued burning of the resin does not permit an excessive temperature to develop in the cask.

9. ACKNOWLEDGEMENT

The fire test was performed at the Naval Damage Control Training Center, United States Naval Base, Philadelphia, Pa. The Training Center permitted us to use a fire basin normally used in teaching the art of extinguishing fuel fires. They also supplied the fuel, ignited the fire, and extinguished it quickly upon our signal. Their cooperation and permission to use their facilities are appreciated.

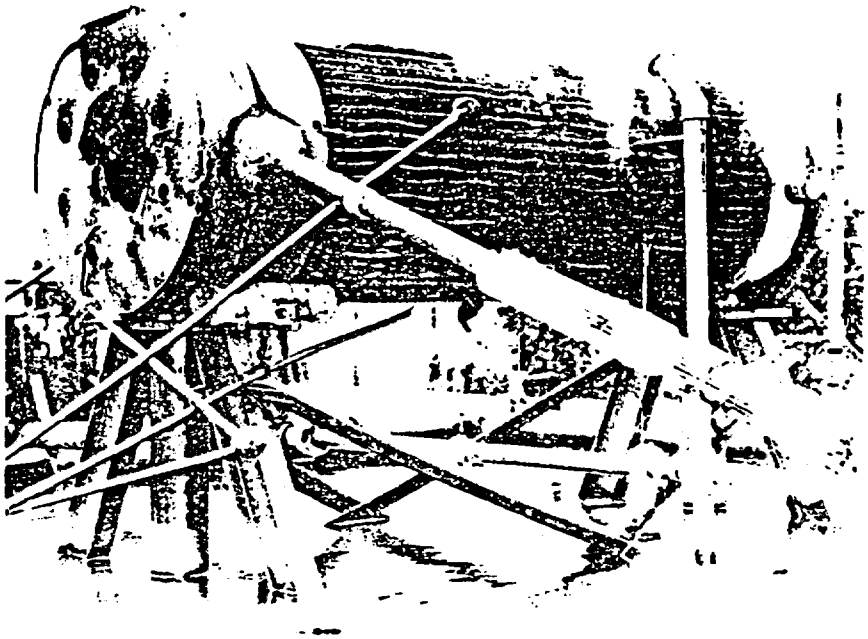

Figure 1

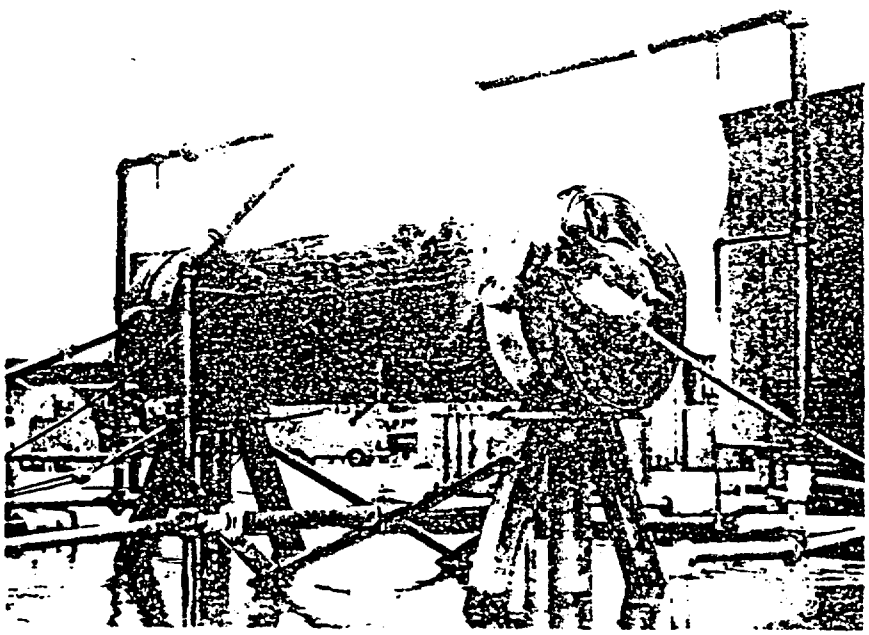

Figure 2

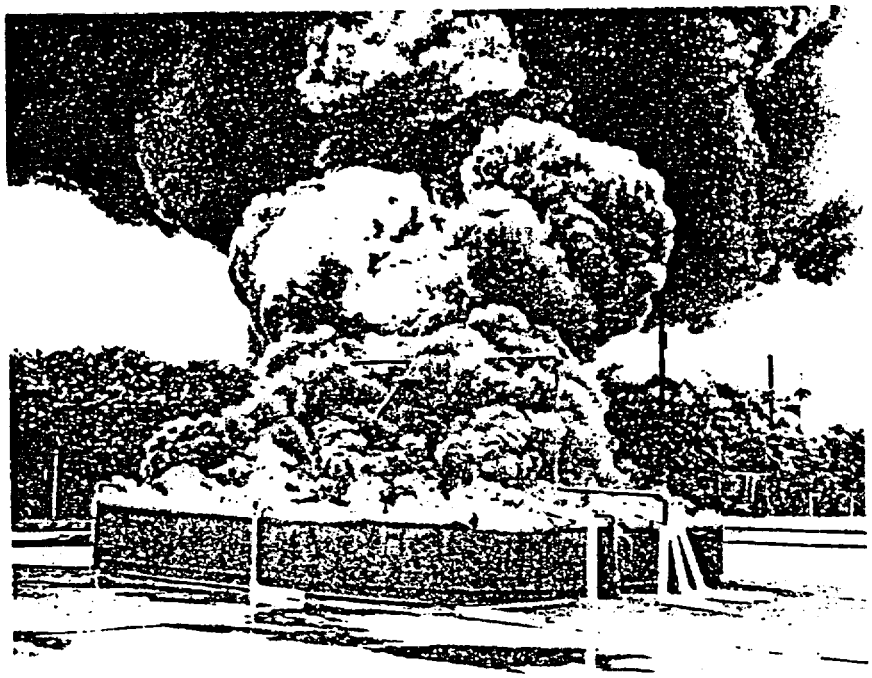

Figure 3

Figure 4

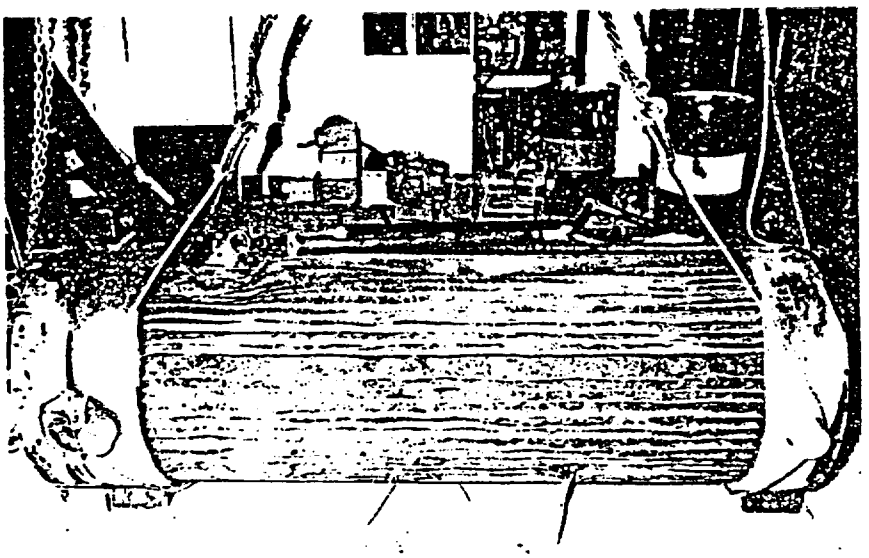

Figure 5

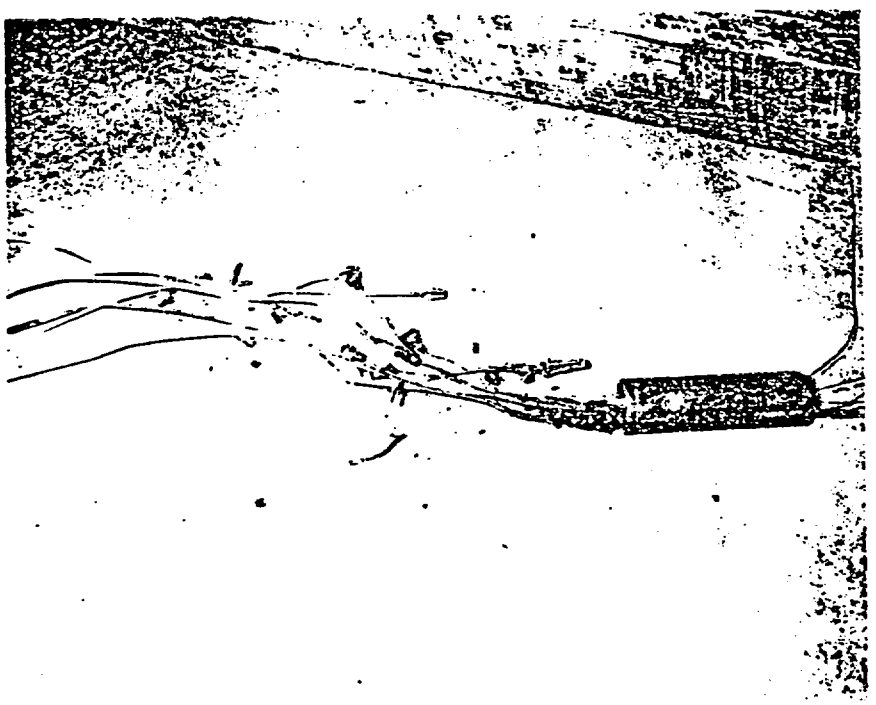

Figure 6

Figure 7

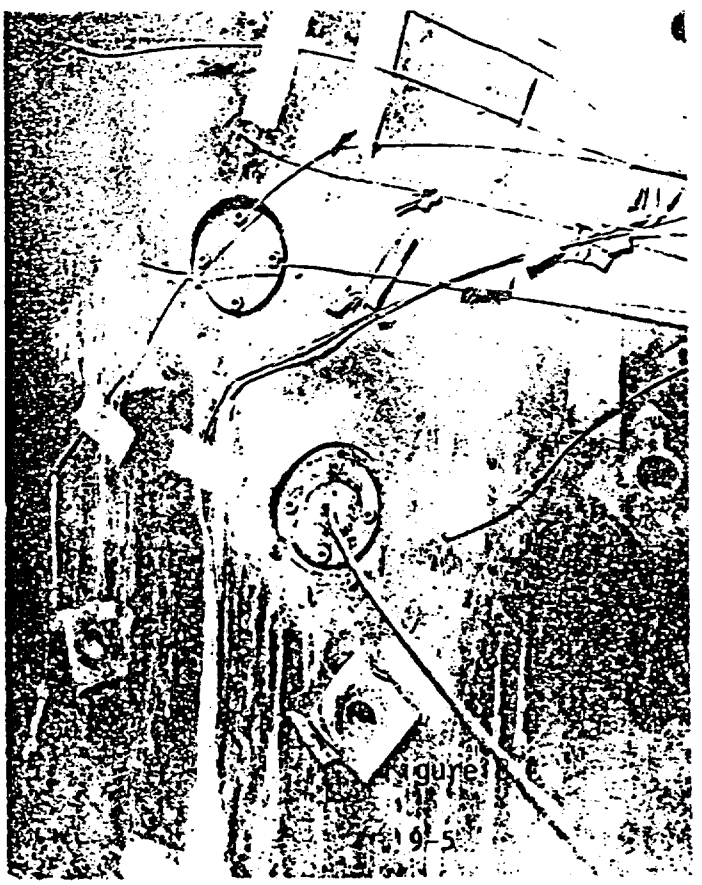

Figure 8

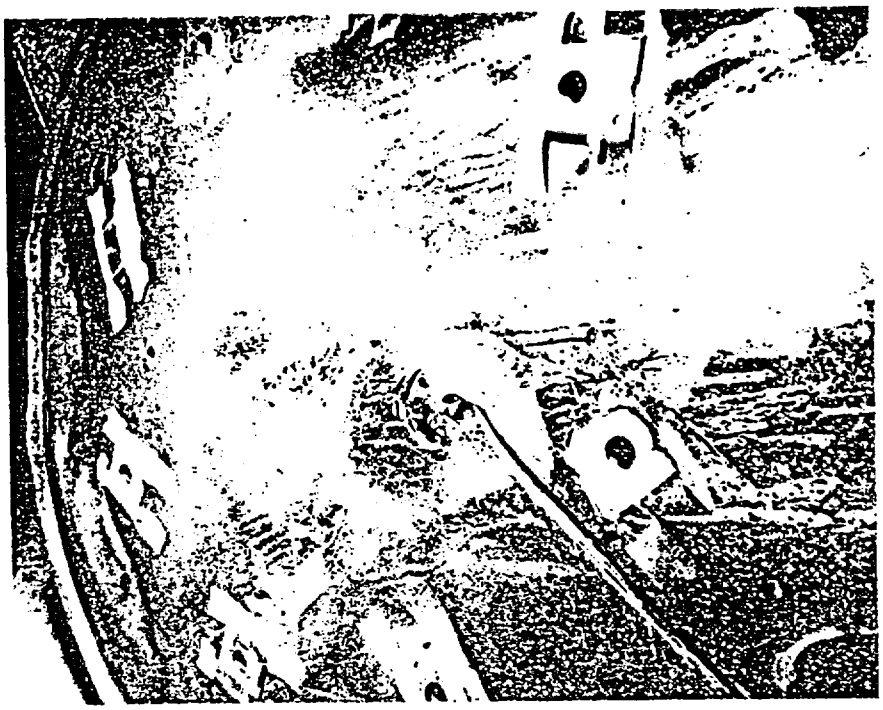

Figure 10

Figure 9

Figure 11

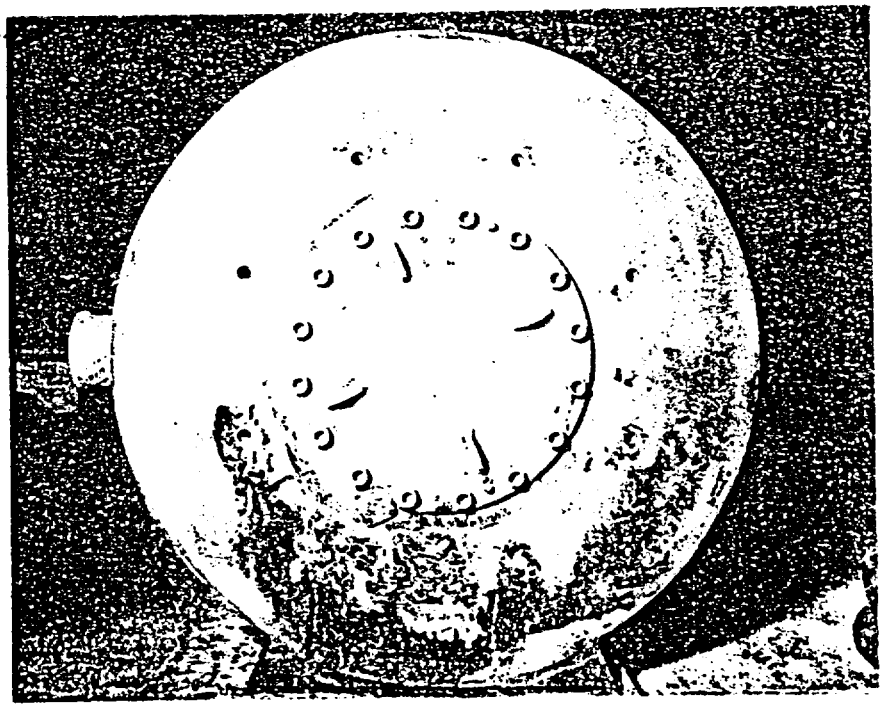

Figure 12

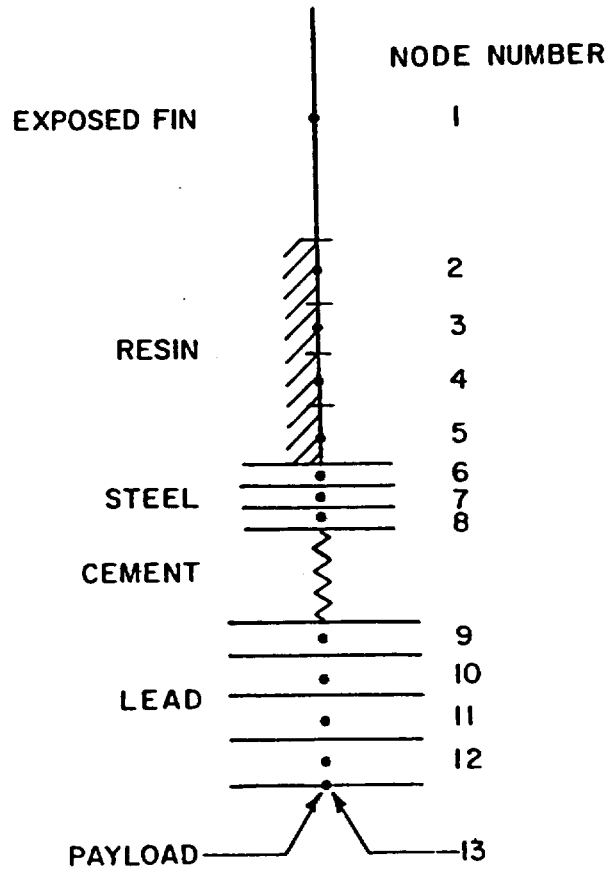

Figure 13. Computational Nodes

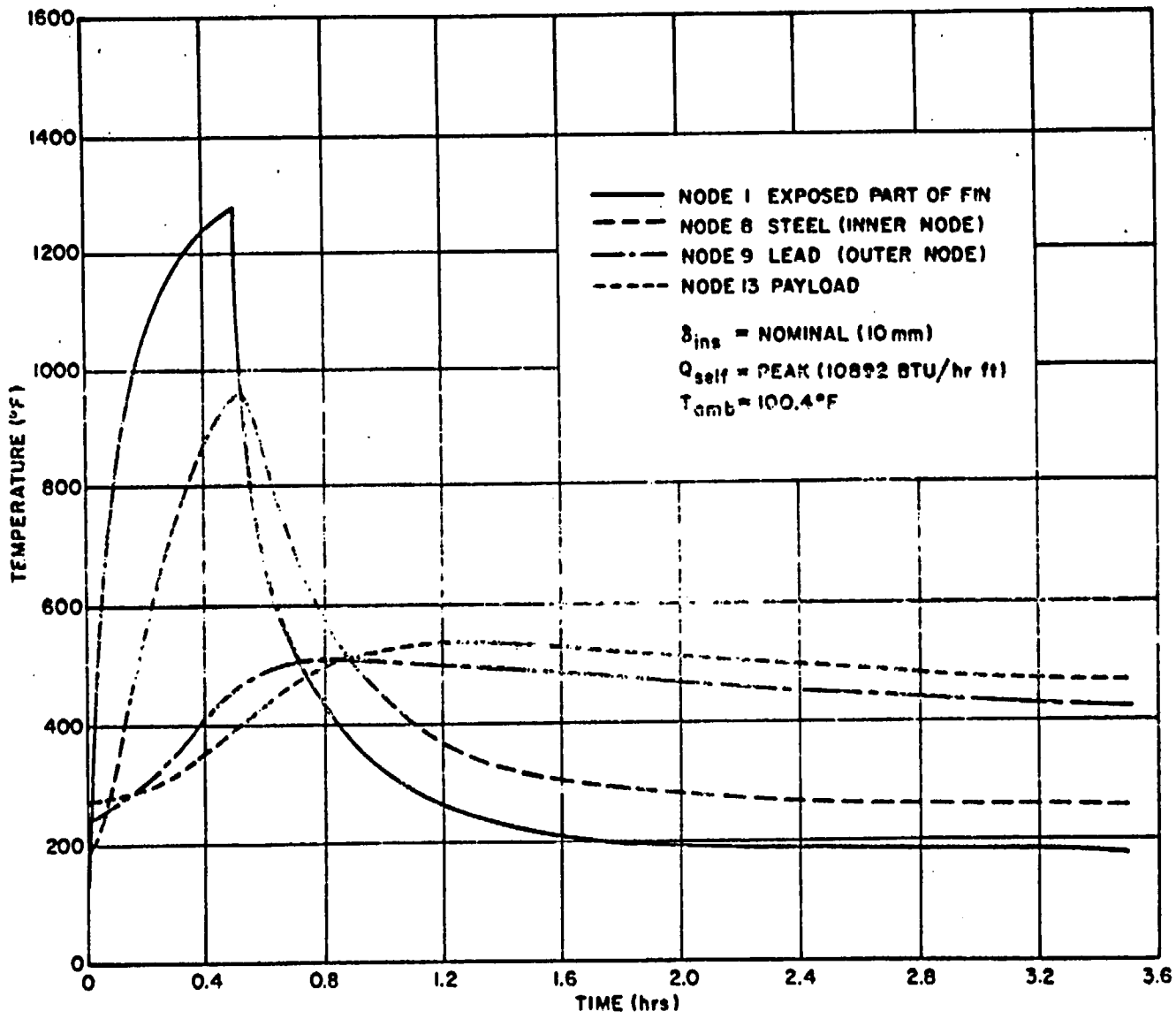

Figure 14. Calculated Full-Scale Thermal Behavior. Temperature Versus Time.

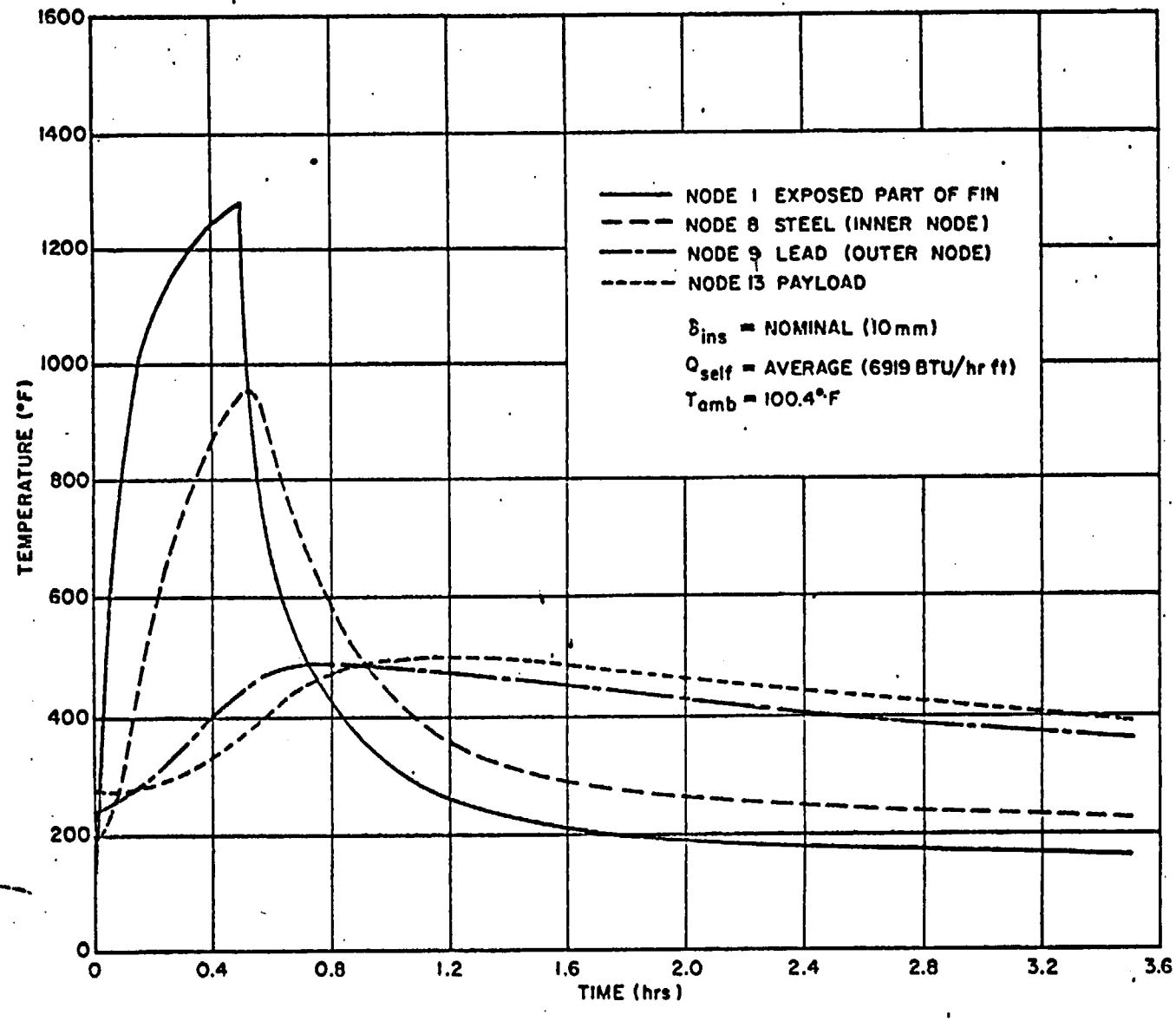

F-C3104-02

Figure 15. Calculated Full-Scale Thermal Behavior. Temperature Versus Time.

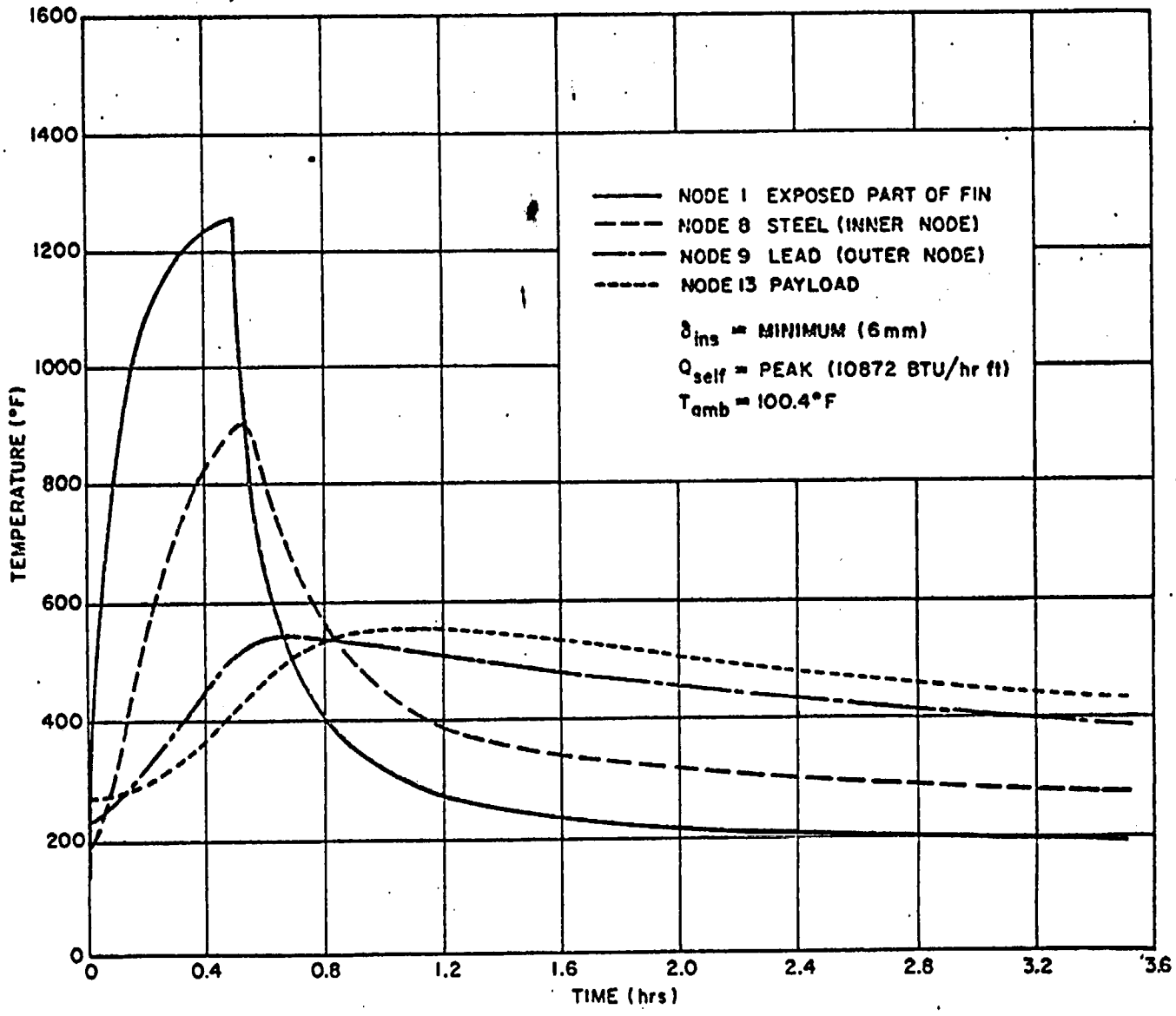

Figure 16. Calculated Full-Scale Thermal Behavior. Temperature Versus Time.

THE FRANKLIN INSTITUTE RESEARCH LABORATORIES

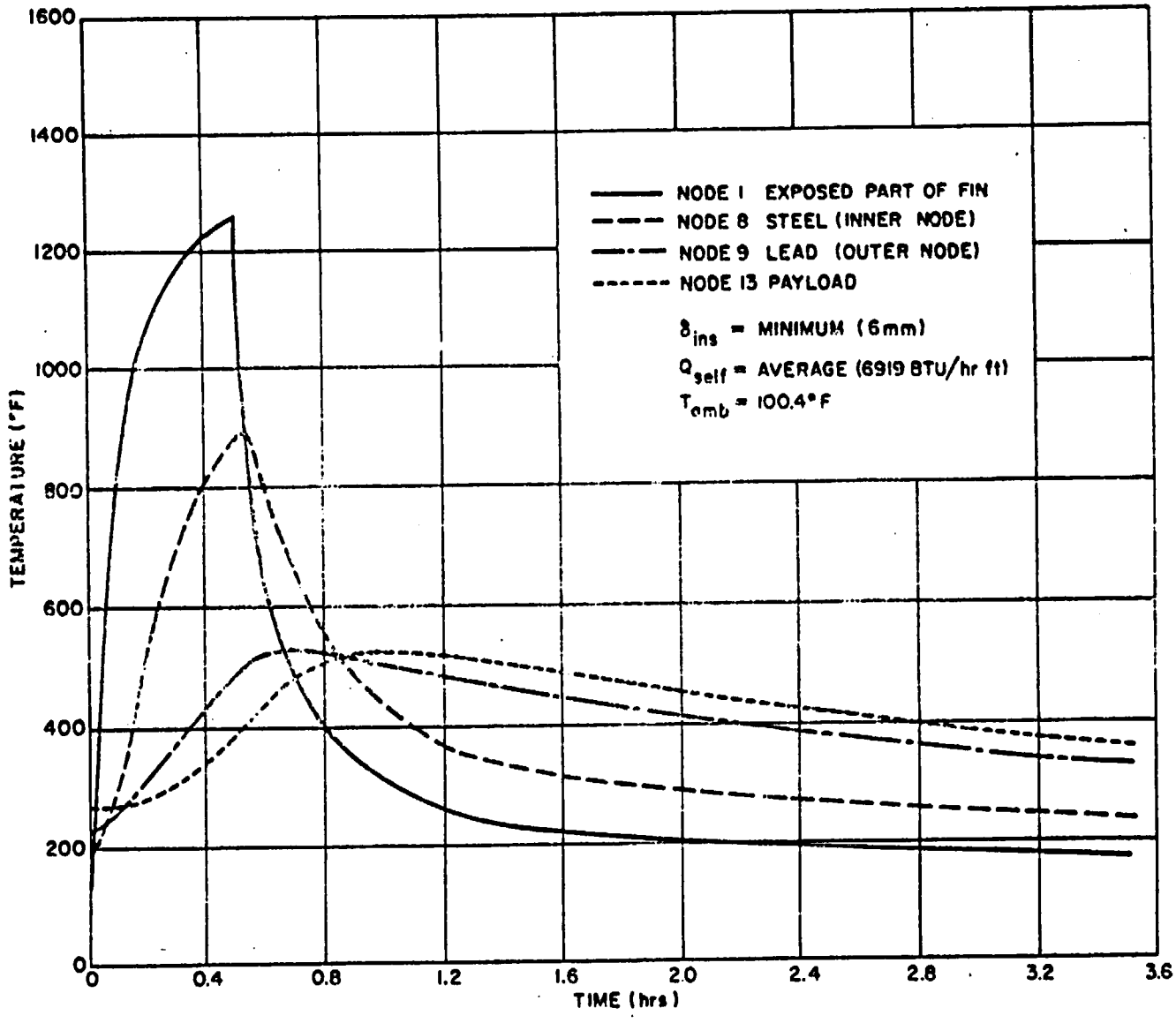

Figure 17. Calculated Full-Scale Thermal Behavior. Temperature Versus Time.

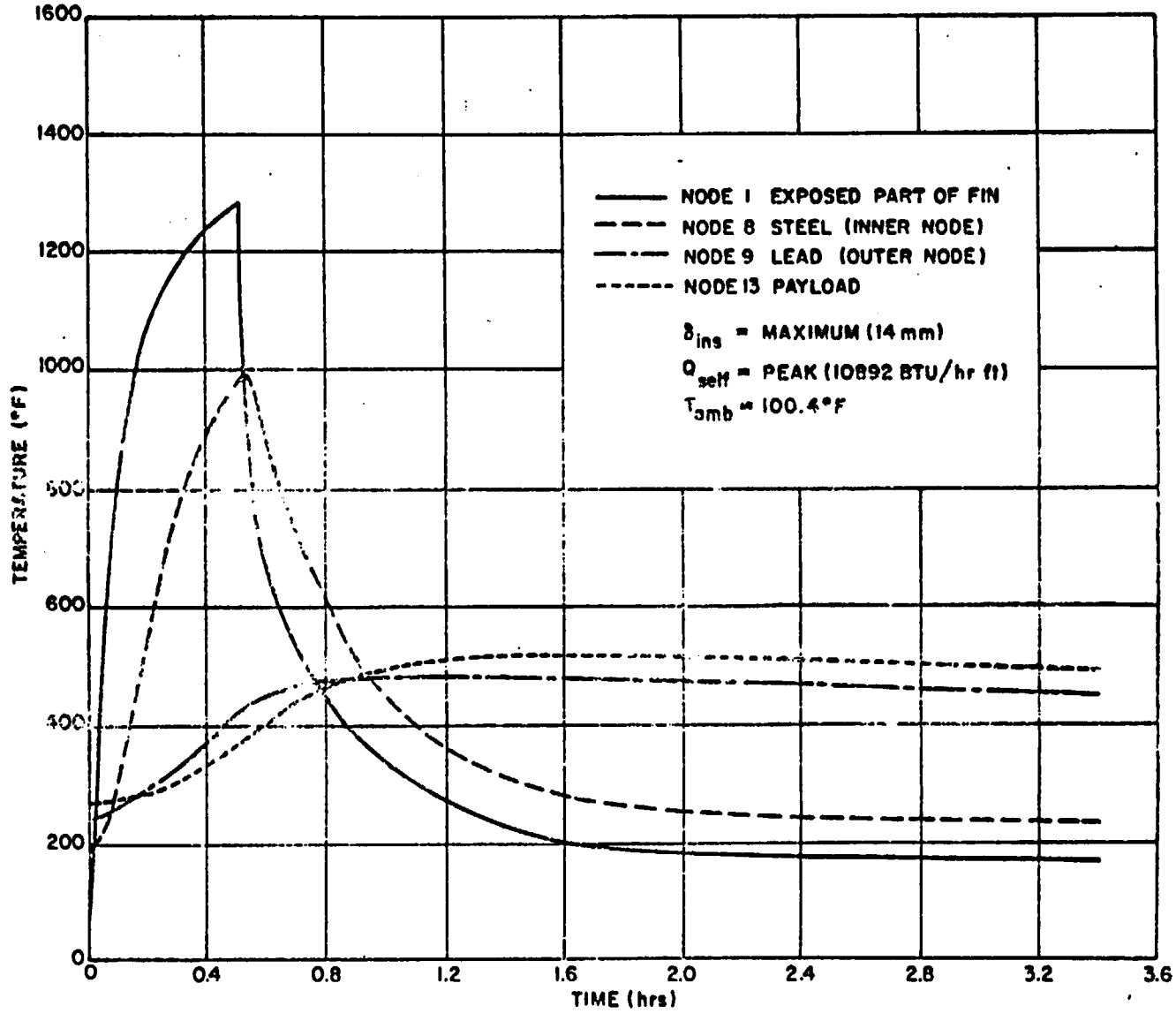

Figure 18. Calculated Full-Scale Thermal Behavior. Temperature Versus Time.

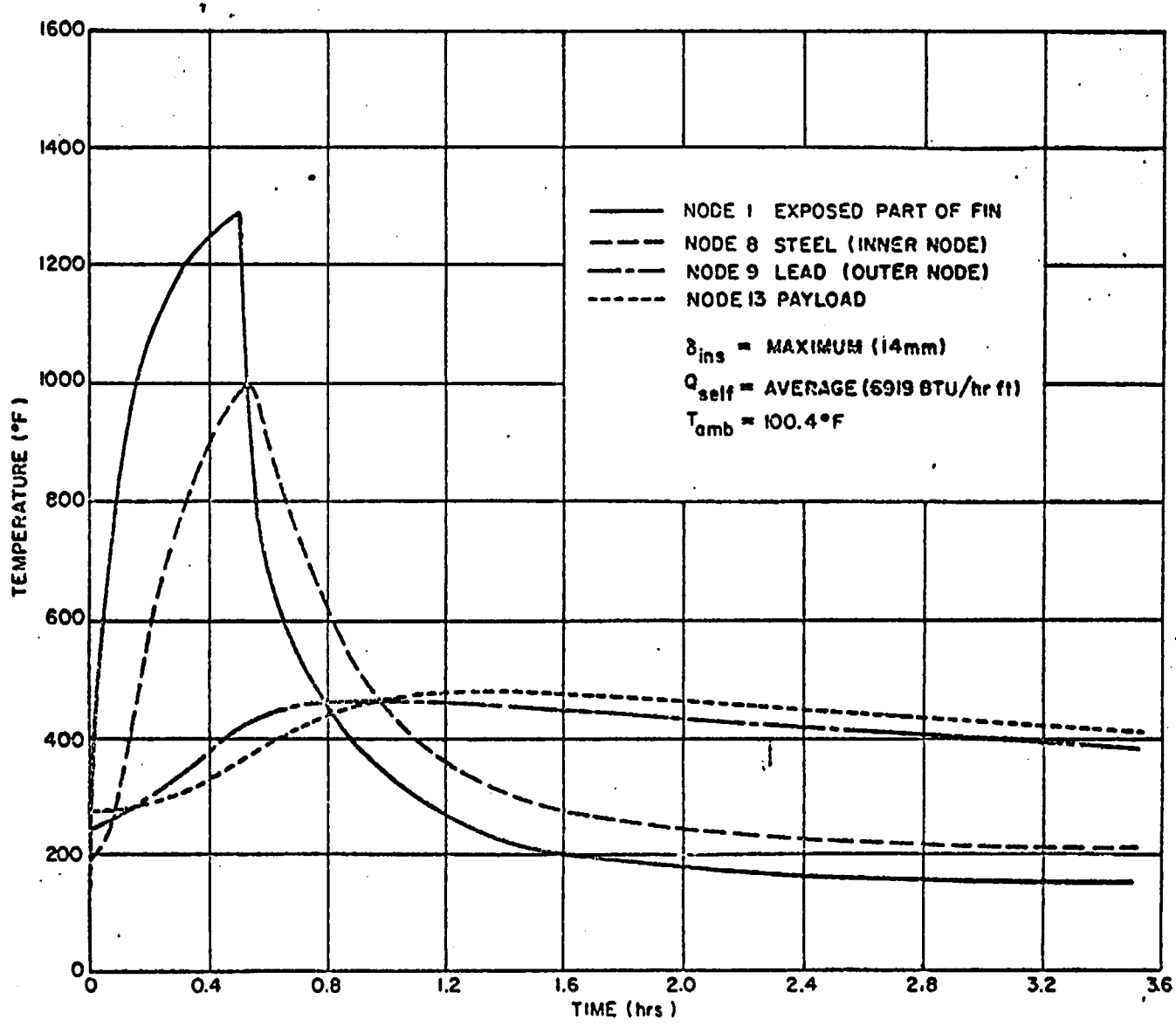

Figure 19. Calculated Full-Scale Thermal Behavior, Temperature Versus Time.

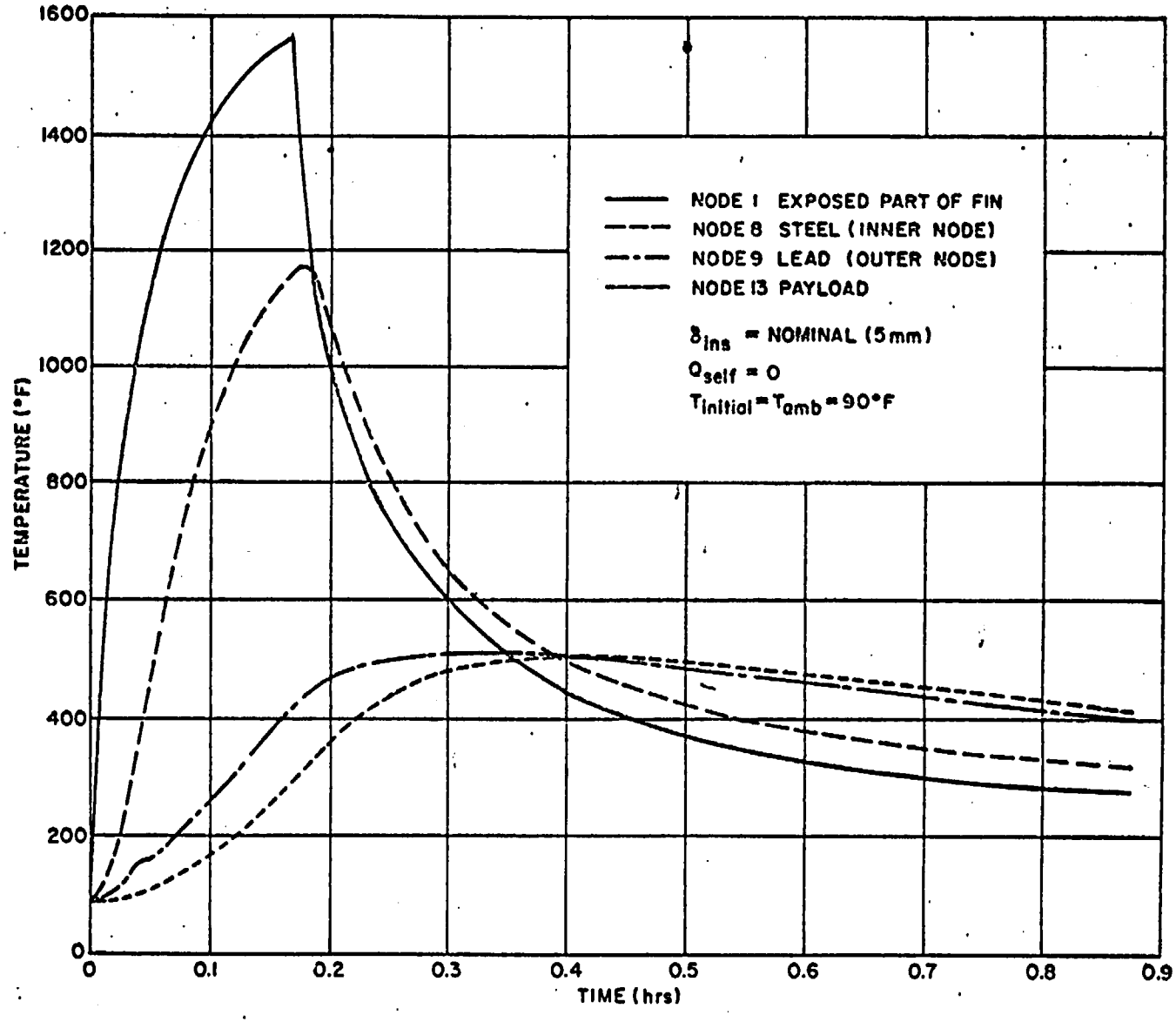

Figure 20. Calculated Thermal Behavior of Model. Temperature Versus Time.

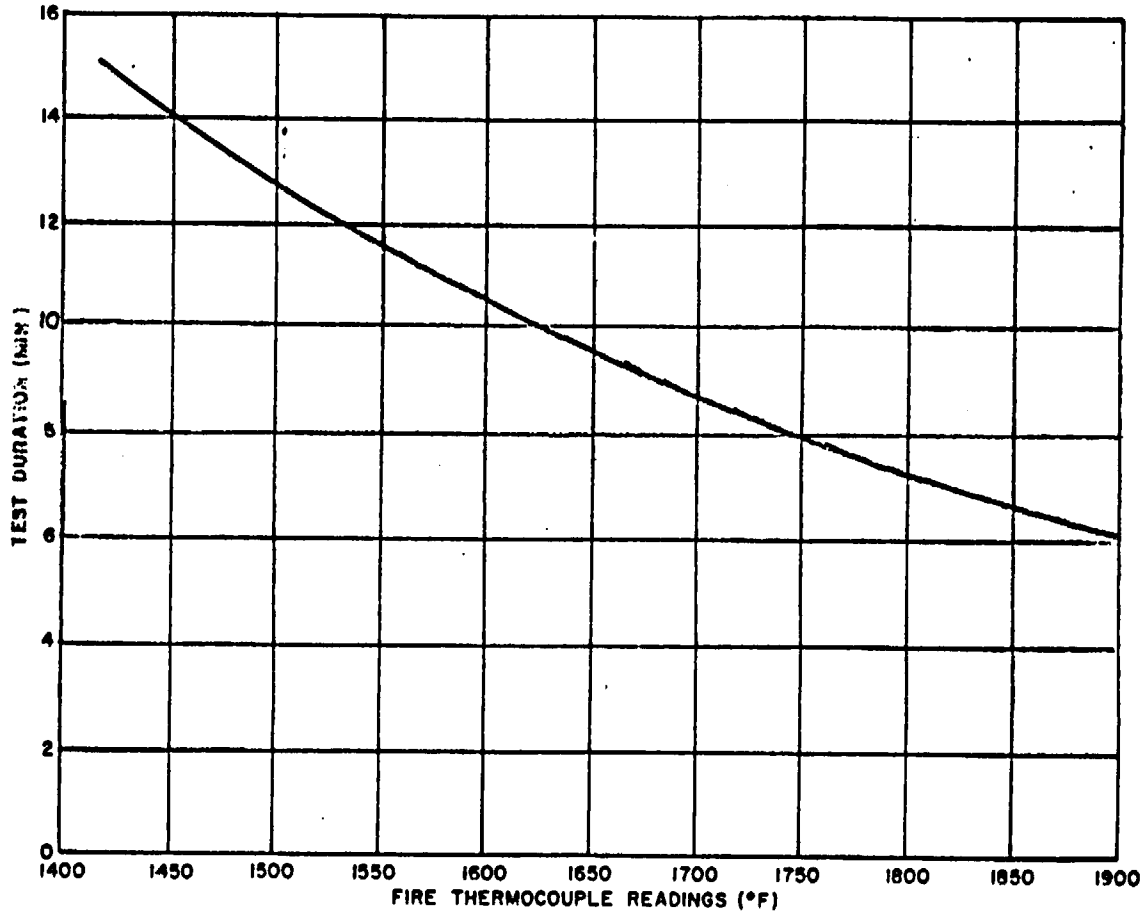

Figure 21. Test Duration Versus Fire Thermocouple Readings

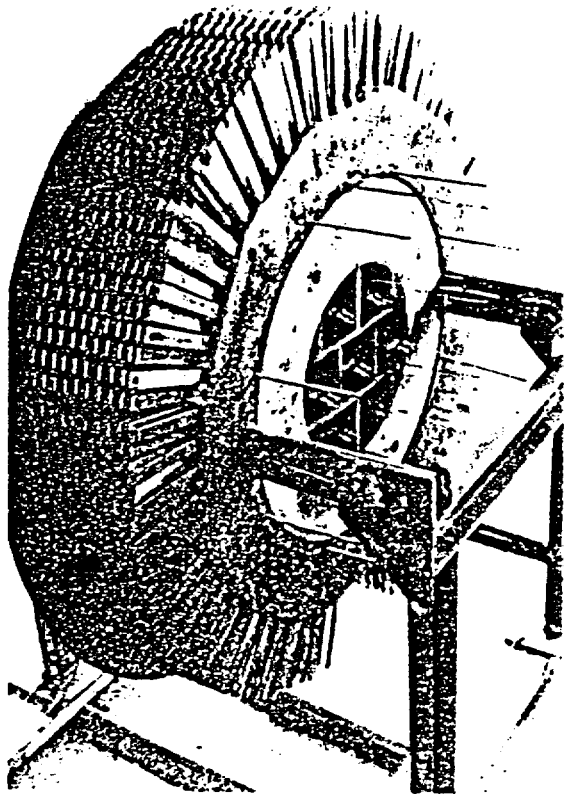

Figure 22. Transnucleaire Full-Scale Model Section.

s.

FIGURE WITHHELD UNDER 10 CFR 2.390

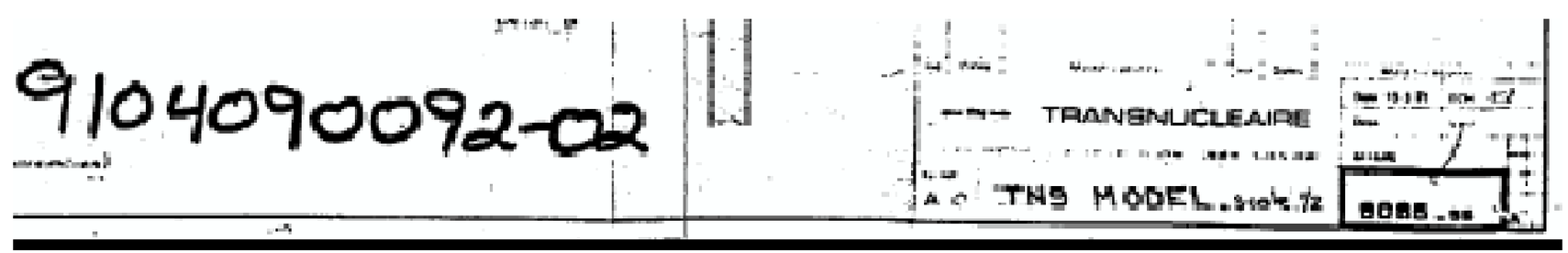

- ANNEX D TO CHAPTER V -

FIRE TEST OF TN9 FULL SCALE SLICE

April 26, 1972

1. INTRODUCTION

The packaging slice already described in Annex A of Chapter IV was submitted to a regulatory open fire test.

Test particulars:

electric power dissipated in model 1,800 W.

duration of fire 30 minutes

beginning of artificial cooling 3 hours after the beginning of regulatory fire

2. BRIEF DESCRIPTION OF FACILITIES

The test was performed at the C.E.A. test station in France. Fire test station facilities include [28]:

- a pit 5 m x 5 m by 2.50 m deep, surrounded by a 1 m high solid steel fence
- 4 trenches for air supply, the flow of which can be adjusted by movable gates
- a fuel pan, 3 m in diameter and 0.300 m deep (approx. capacity 2000 l.)
- temperature recorders
- miscellaneous support equipment

The fire was extinguished by draining the fuel pan.

Fuel oil was used and gasoline was added to facilitate starting.

3. DESCRIPTION OF MODEL (see drawing No. 9085-69)

The model has already been described in Annex A to Chapter IV.

For the purposes of the fire test, it was prepared as follows:

- a fresh veil of cement was cast between the outer shell and the lead;
- supporting legs were extended so that the extremity of the lower fins were at 1 m from the pan bottom and protected by thermal insulation;
- 20 thermocouples Ø 2.3 mm (*) were located as follows:

Ref. 1 (**)	fuel rack (2)
Ref. 2	internal lead surface (4)
Ref. 3	external lead surface (4)
Ref. 4	outer shell inner surface (4)
Ref. 5	outer shell (2)
Ref. 6	ambient atmosphere at 250 mm from the model (4);

- electric heaters were inserted in the fuel rack and generated a total power of 1 800 W. Electrical leads and thermocouple leads were insulated with asbestos;
- the slice was sandwiched between two hollow steel discs filled with rock wool insulation.

(*) Thermocouples were chromel-alumel shielded with stainless steel.

(**) For thermocouple references, see drawing TN No. 9085-69 and fig. 5-D-3.

4. TEST (fig. 5-D-1)

Firing was ignited after thermal equilibrium was reached (electric heating).

The wind speed was between 2 and 3 m/sec. throughout the test.

The initial ambient temperature was 17°C. Within the first minute, the average temperature of ambient atmosphere reached 900°C, then it increased more slowly up to 1027°C.

At the end of a 30 minute fire, the fuel was drained from the fuel pan but no attempt was made to extinguish the resin of the model which continued to burn.

The resin burning rate was about constant for two hours, then began to decrease. At the end of an additional hour water spray was used to extinguish the few remaining sparks.

Curve (6) of fig. 5-D-3 gives the ambient atmosphere temperature profile for the complete test period.

5. RESULTS

Examination of model after test shows that (fig. 5-D-2):

- resin has been transformed into a charcoal-like substance;
- the tips of some of the copper fins melted (about one kilo of copper drops was recovered). Since the melting temperature of copper is 1083°C, we conclude that these fins were exposed to temperatures much higher than those required by the regulations.

- the outside surfaces of the lateral insulation (rock wool) was melted but 3/4 of initial thickness remained intact.
- the cement veil was dried and 1 mm clearance was noticed between the cement and the outer shell along the upper generatrix.
- no evidence of lead melting was noticed. Figure 5-D-3 illustrates the temperature profiles.

We notice that the internal temperatures increase for about 2 -1/2 hours after the end of fire. The outer shell temperatures are maintained between 280°C and 338°C for about 2 hours.

The maximum cement temperature does not exceed 228°C.

The maximum temperature of the inner lead surface is 210°C which is 150°C more than initial equilibrium temperature.

The fuel rack equilibrium temperature increased by 146°C as a consequence of the fire, probably due to:

- dehydration of cement;
- the air gap developed between the outer shell and the veil of cement which causes a distortion of the thermal flux;
- oxidation of copper, melting of some fin tips and local carbonization of resin. The amount melted corresponded to 0.8% of the initial cooling surface.

6. CONCLUSION

The conditions of the fire test were very severe in comparison with regulatory requirements. Nevertheless, the model satisfactorily survived.

Fig. 5.D.1 – *TN9 – Thermal model during open fire test*

Fig. 5.D.2 – *TN9 Thermal model Condition after fire test (lateral insulation removed)*

FIG 5.D3

FIRE TEST OF A IN9 MODEL
RECORDS OF TEMPERATURES

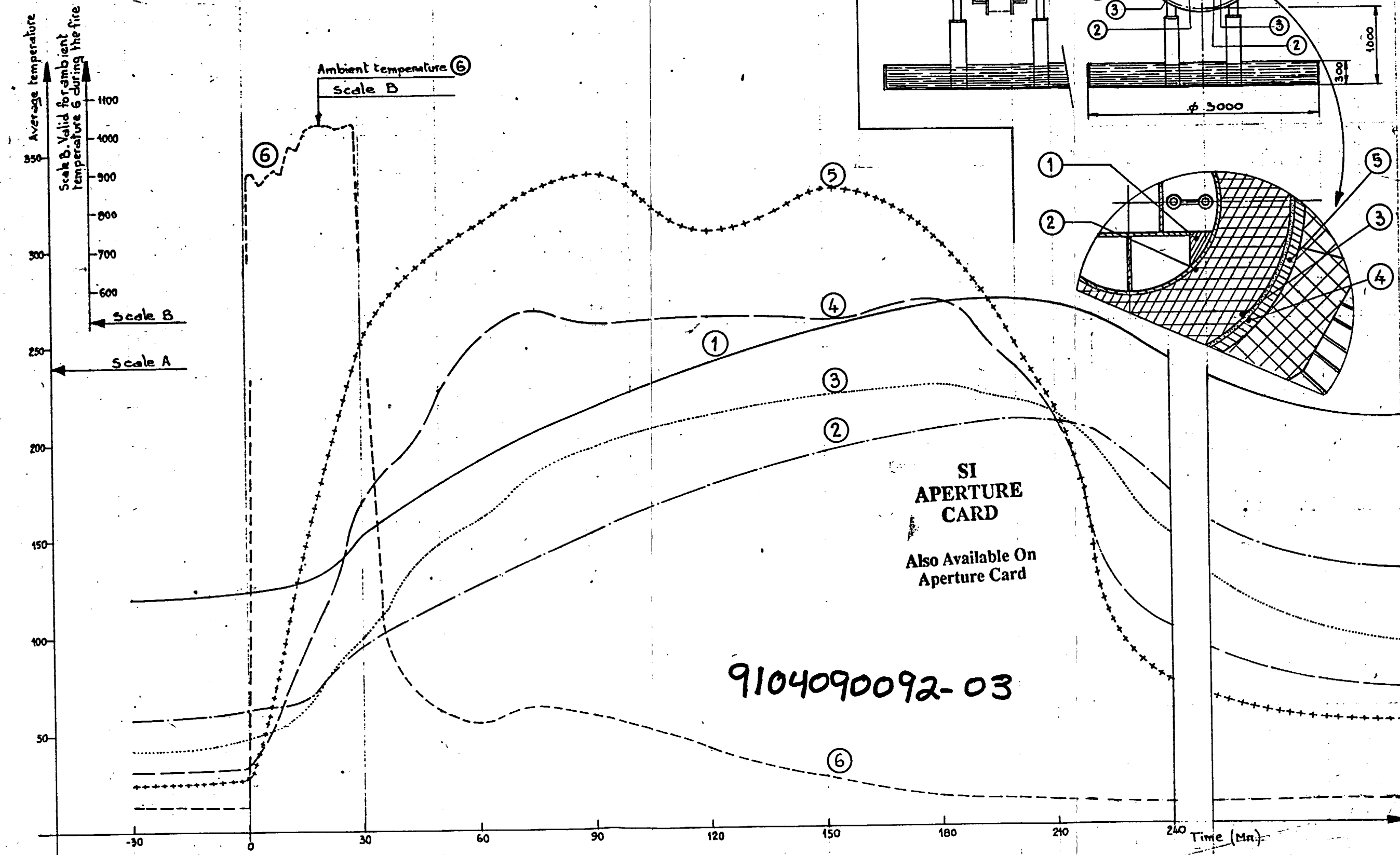

SI
APERTURE
CARD

Also Available On
Aperture Card

9104090092-03

- ANNEX E TO CHAPTER V -
DROP TEST EVALUATION

1. OBJECTIVE

The purpose of this annex is to show that the conclusions of the 9 meter and punch drop tests performed on the package models referred to in Chapter V would not have been changed assuming that these models had incorporated the following design features that were decided subsequent to the tests:

- Reinforced trunnions recessed into the extremity drums and protected by protruding removable impact limiters
- Drain orifice laterally recessed in the extremity drum instead of located on the bottom plate
- Inner basket of the TN9 replaced by a compartment structure similar to that of the TN8
- Reduction of the number of fins for the TN-8L.

2. HORIZONTAL DROP OF 9 METERS ON THE TRUNNIONS

2.1 Behavior of the TN9 cask half-scale model

That model is represented on Drawing TN 9085-55 (Page 258). As indicated in Annex B to Chapter V, the apparant damages after the horizontal drop on trunnions concerned only these trunnions without significant deformation of the extremity drums or bending of the cask model body (see Fig. 5.B.5) and the peak deceleration was 180 g.

The deformed trunnions were removed to allow the cask model to be refurbished by the BAM* for additional drop tests. This permitted us to observe that the inner trunnion segments did not suffer apparent damages. We also verified by examining the high speed.

*Bundesanstalt fur Materialprufung, Berlin, Germany

motion pictures taken during the drop that the cask rotational energy during the bounce after the drop may be neglected as it represents less than 0.5 % of the drop energy.

Therefore, we may conclude that practically the whole drop energy was dissipated during the compression of the protruding segments of the trunnions (made of carbon steel).

2.2. Trunnion modifications subsequent to the tests of the TN9 cask half-scale model

The attachment of the trunnion to the outer shell is reinforced and rigidified by enlarging the section thickness of the trunnions, adding gussets and reducing the length of the trunnion inner segment.

The outer segment of the trunnions is reinforced and no longer protrudes from the extremity drums. Their extremities are provided with removable impact limiters which protrude the extremity drums as the trunnions of the former design.

The deformable part of these impact limiters is dimensioned as that of the former trunnions (diameter : 160/200 mm, length : 150 mm). The material is also the same (carbon steel).

2.3. Behavior of the modified trunnions equipped with impact limiters

As the impact limiters fastened to the extremities of the trunnions of the TN8/TN9 models have the same geometry and same resistance as the trunnions of the half-scale model, we may anticipate that they will similarly absorb the whole drop energy without significant damage to other parts of the model. We also may consider that the peak deceleration will not exceed 90 g, taking into account the scale factor correction.